

## Response to the comments of Anonymous Referee #1

(Referee comments in black, our responses in blue)

Referee general comment 1:

DeRieux et al. present an extension of their recent model that predicts the viscosity of organic aerosol particles as a function of their simplified chemical composition, using elemental ratios. They have extended the model, largely using data recently compiled by Rothfuss and Petters (2017), to include organics with a molar weight up to ~1100 g/mol, from the original 450 g/mol. The motivation for this work is to predict the diffusivity of organic aerosol, as this /may/ have important limitations for vapor uptake and growth, water uptake and CCN activation, equilibration timescales, etc. It is important to note that this model only estimates the glass transition temperature, from which viscosity can in turn be estimated, and from this an estimate of diffusivity can be made. So, there are many critical steps along the way to deriving the actual property of interest, and the uncertainties involved in each of these steps needs to be discussed fully in this manuscript. Following the careful clarification and further discussion of several important aspects in this manuscript it should be acceptable for publication in ACP. The topic is within scope though personally I think there has been an over-abundance of effort spent recently on viscous organic aerosols. The significance and novelty of the research presented here is quite low by ACP standards, as it merely extends a recent model, and the model's predictions involve an important series of significant assumptions and estimations, and yet the actual diffusivity is still not arrived at. If I was interested in predicting viscosity or diffusivity I personally would turn to Rothfuss and Petters' functional group-based method. It provides deeper chemical insight, since viscosity and diffusivity are created by the interactions between molecules and their functional groups/dipoles. Still, if the major issues with this method and manuscript are satisfactorily addressed, there is nothing technically wrong with this paper to prevent its publication. I do think the authors could be addressing this topic in a deeper and more comprehensive way, and I hope my comments can be used to improve the paper. Referee #2 also raised several excellent points that also need to be fully addressed.

Thank you for your comments. While we acknowledge the importance of the diffusion coefficient, the primary purpose of this paper is to predict the glass transition temperature and viscosity for SOA mixtures using a bottom up approach (as specified in title, abstract and throughout the text) that can be used to make predictions of viscosity from soft-ionization high-resolution mass spectrometry data and be incorporated into atmospheric models. We are fully aware that estimations of bulk diffusivity involve multiple steps and that the Stokes-Einstein equation can be used for conversion of viscosity to bulk diffusivity for first-order approximation, but this relation may break down in highly viscous systems (Power et al., Chem. Sci., 2013; Marshall et al., Chem. Sci., 2016; Chenyakin et al., 2017). Bulk diffusion of small molecules such as water and ozone should be treated separately, for example using obstruction theory or percolation theory (e.g., Shiraiwa et al., PNAS, 2011; Bones et al., PNAS, 2012; Berkemeier et al., ACP, 2014; Price et al., ACP, 2015). In this study, we focus on estimations of  $T_g$  and viscosity. Estimations of bulk diffusivity in the SOA material are beyond the scope of this study.

We agree that the functional group model by Sastri and Rao (1992), as used by Rothfuss and Petters (2017), is a valuable method to predict the viscosity of a single pure organic compound when the chemical structure is known. Rothfuss and Petters (2017) demonstrated the influence of functional groups on viscosity of pure organic compounds, but did not provide a method to predict viscosity of complex multi-component SOA mixtures. In addition, the chemical structures of SOA components are often not known, whereas their elemental formulae can be determined in HR-MS measurements, and our method is able to provide practical estimates of  $T_g$ , making use of these measurements. Also, there are not yet any regional or global air quality models that explicitly treat functionality of SOA compounds. On the other side, the viscosity estimation method presented in our work is applicable in a global model (e.g., Shiraiwa et al., 2017) and the  $T_g$  prediction method developed in this study can be practically applied for example in the SOM model (Cappa and Wilson, 2012; Jathar et al., 2015). Thus, we are confident that this study is valuable and it would merit publication in ACP.

Comment 2: Introduction (page 3-4): The potential importance of viscous organic aerosol phases is really over stated here. As many other papers have done, most of the important implications of viscous organics are predicted but few have actually been demonstrated through laboratory or ambient experiments using real complex atmospheric aerosol or reasonable proxies. The authors are cherry picking the results to motivate their work. For example, the slow evaporation of SOA referred to is observed after a significant fraction of the SOA promptly evaporated. The slowly evaporating SOA remaining cannot be distinguished from the effects of diffusional limitations or just being too darn low in volatility. The viscosity of alpha-pinene SOA was recently studied in a more direct manner using optical tweezers and no significant limitations to diffusion were reported (Gorkowski et al., 2017). The authors are also ignoring highly relevant novel experiments from Neil Donahue's group where they use aerosol population experiments to evaluate the very condensation growth limitations that these authors posit are an important consequence of viscous SOA. Yet Ye et al. did not observe impediments to mixing expect at quite low RH (Ye et al., 2016). Scot Martin's group has approached this topic from a different perspective (Liu et al., 2016). And I see Ye et al. has extended these experiments to study toluene and some other systems as well: Ye, Q., Upshur, M. A., Robinson, E. S., Geiger, F. M., Sullivan, R. C., Thomson, R. J. and Donahue, N. M.: Following Particle-Particle Mixing in Atmospheric Secondary Organic Aerosols by Using Isotopically Labeled Terpenes, *Chem*, doi:10.1016/j.chempr.2017.12.008, 2018. The authors need to present the motivation behind studying viscous aerosol phases in a more precise and balanced manner, distinguishing between those effects that have been speculated, and those for which there is actual significant experimental evidence (especially from realistic atmospheric aerosol). Here for example is an interesting documented effect of phase state causing differential growth of aerosol particles: Zaveri, R. A., Shilling, J. E., Zelenyuk, A., Liu, J., Bell, D. M., D'Ambro, E. L., Gaston, C. J., Thornton, J. A., Laskin, A., Lin, P., Wilson, J., Easter, R. C., Wang, J., Bertram, A. K., Martin, S. T., Seinfeld, J. H. and Worsnop, D. R.: Growth Kinetics and Size Distribution Dynamics of Viscous Secondary Organic Aerosol, *Environ. Sci. Technol.*, 52(3), 1191-1199, doi:10.1021/acs.est.7b04623, 2018.

Following the reviewer's suggestion, we have extended the introduction to discuss previously missed relevant studies as indicated below:

*Lines 56-59: "SOA particles were observed to evaporate unexpectedly slowly (Cappa and Wilson, 2011; Vaden et al., 2011), and recent modeling studies have evaluated the contributions of low diffusivity and volatility to slow evaporation rates (Roldin et al., 2014; Yli-Juuti et al., 2017)."*

*Lines 79-88: "Partitioning of semi-volatile compounds into viscous particles may result in kinetically-limited growth in contrast to quasi-equilibrium growth (Perraud et al., 2012; Shiraiwa and Seinfeld, 2012; Booth et al., 2014; Zaveri et al., 2014; Mai et al., 2015; Liu et al., 2016), which also affects the evolution of particle size distribution upon SOA growth (Shiraiwa et al., 2013; Zaveri et al., 2018). Chamber experiments probing mixing timescales of SOA particles derived by oxidation of various precursors such as isoprene, terpene, and toluene have observed strong kinetic limitations at low RH, but not at moderate and high RH (Loza et al., 2013; Ye et al., 2016; Ye et al., 2018). Gorkowski et al. (2017) did not observe significant diffusion limitations for glycerol and squalene in  $\alpha$ -pinene SOA. Quasi-equilibrium versus kinetically-limited or non-equilibrium SOA growth remains an open issue and warrants further investigations. "*

Comment 3: Page 3: Particle bounce measurements are not a reliable assessment of viscosity, and certainly not of diffusivity. These measurements may have started the focus on viscous phases but the measurement methods have advanced considerably since then. What we really need are measurements of the diffusivity of different types of molecules in atmospheric aerosols.

Even though bounce experiments do not provide robust viscosity measurements, they can give useful insights into the particle phase state and provide rough estimates of viscosity (Bateman et al., 2014; Bateman et al., 2015). As such, the results from these studies are represented with shaded boxes in our figures to represent the estimated viscosity. Additionally, we strongly agree that direct measurements of bulk diffusivity are needed (Chenyakin et al., 2017).

Comment 4: Line 59: Truly direct measurements of viscosity are difficult to achieve with the small mass loadings of aerosol available. Were these truly "direct" measurements of viscosity? More likely they were inferred from poke-flow or bead transport measurements.

In the references cited at Line 59, viscosities were inferred from measurements, such as poke-flow measurements, beam mobility measurements, and fluorescence lifetime imaging measurements. To address the referee's comment, "direct" will be removed from Line 59.

Comment 5: Line 70: It is odd that the important plasticization effects of water vapor uptake are not mentioned anywhere near this section on retarded water vapor uptake. Water uptake will reduce viscosity and these transport limitations.

We are fully aware of the plasticizing effect of water and we consider hygroscopic growth and use the Gordon-Taylor approach to account for this effect. We have clarified this point in the revised manuscript by adding the following text:

*Lines 50-51: “The phase state is also strongly affected by relative humidity, as water can act as a plasticizer to lower viscosity (Mikhailov et al., 2009).”*

*Lines 226-228: “SOA particles contain a number of organic compounds as well as a variable amount of liquid water, which has low  $T_g$  (136 K) and can act as a plasticizer (Mikhailov et al., 2009; Koop et al., 2011).”*

Comment 6: Line 73: Effects of slow water uptake on ice nucleation properties is one of those effects that has been proposed but I do not think there is direct evidence for this. Certainly not in realistic complex aerosol particles.

Direct experimental evidence for the effect of slow water uptake on ice nucleation properties has been reported by multiple groups for model organic compounds (Murray et al., 2010; Schill et al., 2014), laboratory generated SOA (Wang et al., 2012a; Ignatius et al., 2016; Charnawskas et al., 2017), and ambient SOA particles (Wang et al., 2012b). A comprehensive review on this topic was published very recently (Knopf et al., 2018). We have added additional references in the revised manuscript.

Comment 7: Line 89: The highly related study by Rothfuss and Petters really warrants much further discussion here. Their paper significantly advanced the methods we can use to understand and predict viscosity and diffusivity, and did this from a functional group perspective. This manuscript also borrows heavily from the extensive dataset compiled by Rothfuss and Petters, and that paper deserves more credit for enabling the modeling presented in this manuscript under consideration. Later in this paper there also needs to be a solid comparison of this model to the functional group based one of Rothfuss and Petters.

We agree that the functional group model by Sastri and Rao, as used by Rothfuss and Petters, is a valuable method to predict the viscosity of single pure organic compound when the functional groups and structure of that compound are known. However, such an approach does not include a method for determining  $T_g$  or viscosity of multi-component mixtures (Rothfuss and Petters, 2017). To direct readers to their valuable work, we have added the following statement to our manuscript.

*Lines 89-91: “Group contribution methods have been used to predict the viscosities of pure compounds when the functionality and molecular structure are known (Sastri and Rao, 1992; Rothfuss and Petters, 2017).”*

*Lines 98-99: “These studies provide important insights in estimating the viscosity of individual organic compounds.”*

Comment 8: Line 98: This is an inaccurate statement; we are getting more and more molecular-level understanding of organic aerosols and their vapor precursors, such as

from CIMS, and also FT-IR, Raman, and other analysis methods. While molecular-based analysis is more challenging than just reducing the measurements to simple elemental ratios, molecules can still be measured, they are what matter, and this is not a valid justification for relying on HCO ratios. You could refer to the large existing datasets from the AMS for example that only reduce the organic aerosol to its elemental ratios as a motivation for an atomic ratio-based model.

We have deleted this sentence in the revised manuscript.

Comment 9: Section 2: I have a series of concerns regarding how viscosity is measured here. The uncertainties in the various parameters and estimates involved need to be properly discussed, and these uncertainties propagated to provide an uncertainty range for the actual estimate of viscosity. The parameterization begins with an estimate of the melting point,  $T_m$ , from the EPA EPI Suite. Then the glass transition point,  $T_g$ , is estimated from  $T_m$ . How accurate are these estimates, especially for the types of molecules relevant for atmospheric aerosol? Was the EPA model trained on these sorts of models? Or you not use  $T_m$  in this new model since Eqn. (2) does not depend on  $T_m$ ? In the end you state that Eqn. (1) can only be used for  $M < 450$  g/mol but Eqn (2) is not suitable for use in common models such as the VBS. Since Eqn (1) will still be used these important aspects regarding the uncertainties in  $T_m$  and  $T_g$  need to be clarified.

Please note that both Eq. (1) and (2) are developed based on experimental  $T_g$  data. Eq. (1) is developed based on 178 CH and CHO compounds with measured  $T_g$  compiled by Koop et al. (2011) plus 3-methylbutane-1,2,3-tricarboxylic acid (3-MBTCA), an atmospheric oxidation product of  $\alpha$ -pinene with its measured  $T_g$  of  $305 \pm 2$  K (Dette et al., 2014). Eq. (2) is developed based on the above 179 compounds plus the experimental  $T_g$  data compiled in Rothfuss and Petters (2017).

As measurements of  $T_g$  for atmospheric SOA components are scarce (Dette et al., 2014), as shown in Fig. 1c in the manuscript, we validate our parameterization by comparing the  $T_g$  predicted by Eq. (2) (referred as “predicted  $T_g$ ”) with both measured  $T_g$  (Koop, et al., 2011; Dette et al., 2014; Rothfuss and Petters 2017) as well as estimated  $T_g$  for 654 SOA components following the Boyer-Kauzmann rule with their melting temperature  $T_m$  (referred as “estimated  $T_g$ ” in our manuscript), which has been validated by Koop et al. (2011). Thus, the Boyer-Kauzmann rule is used with an attempt to validate the ability of Eq. (2) applied in atmospheric organic components. The new figure Fig. A2(a) shows that the Boyer-Kauzmann rule works well to estimate  $T_g$ . For the 654 SOA components (Shiraiwa et al., 2014), as shown in Fig. 1c in the manuscript, even though  $T_m$  from the EPI Suite is adopted (because the measured  $T_m$  are not always available), Eq. (2) can constrain those compounds reasonably well. Regarding the uncertainty in  $T_g$  predictions, as we wrote in the manuscript,  $T_g$  of individual compounds can be predicted within  $\pm 21$  K as indicated by the prediction band (dotted lines in Fig. 1c).

In short summary, both Eq. (1) and (2) are developed based on experimental  $T_g$  and the Boyer-Kauzmann rule estimating  $T_g$  by  $T_m$  is only used for comparison with Eq. (2) predictions. We agree with the reviewer’s note that Eq. (1) can be applied in the VBS more easily. As we wrote in the manuscript, regarding the application in aerosol models, Eq. (2) may be suitable for coupling with the statistical oxidation model which

characterizes the SOA evolution as a function of  $n_C$  and  $n_O$  (Cappa and Wilson, 2012; Jathar et al., 2015). Eq. (2) is more flexible than Eq. (1) to bring in the compounds containing hetero-atoms (e.g., nitrogen or sulfur) in future studies.

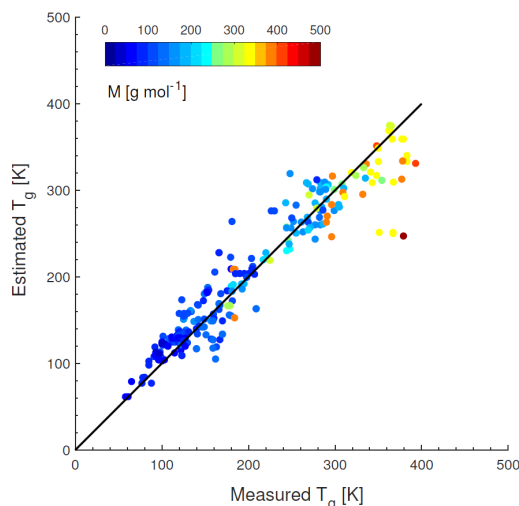


Figure A2(a). Comparison of measured and estimated  $T_g$  by the Boyer-Kauzmann rule for 251 organic compounds (Koop et al., 2011; Dette et al., 2014; Rothfuss and Petters 2017) with their measured  $T_m$  available. The markers are color-coded by molar mass.

Comment 10: Line 200: Please explain the free volume theory and topological constraint theory. Line 288: Please explain and justify the free volume assumption.

We have further explained these concepts by revising our manuscript as follows:

Lines 200-207: “The correlation between  $T_g$  and the number of carbon atoms is consistent with the free volume theory, in which molecular motion is restricted by the difference between the space required for a molecule to vibrate versus the space in which the molecule resides (i.e. the free volume) (White and Lipson, 2016). The correlation between  $T_g$  and the number of OH groups is more consistent with the topological constraint theory where the primary influence is the three dimensional structure of the molecule as determined by such factors as molecular bonds and hydrogen-bonding networks (Nakanishi and Nozaki, 2011; van der Sman, 2013).

Comment 11: Page 240: “Water mass fraction can be estimated using the effective hygroscopicity parameter”. This likely will not capture the small but important mass fraction of water uptake at low RH that leads to significant plasticization and reduction of viscosity. You need to discuss if there is experimental evidence supporting the use of growth factor derived water uptake measurements to describe the effects of water on  $T_g$  and viscosity.

We have added the following discussion in the revised manuscript as follows:

Lines 245-249: “Pajunoja et al. (2015) found that water uptake in subsaturated conditions is inhibited until RH is high enough for dissolution of water in SOA particles with relatively low O:C ratios. As oxidation of SOA increases, solubility of water

*increases and dissolution occurs at lower RH values. In both cases, the use of subsaturated hygroscopicity measurements was supported.”*

*Lines 227-229: “SOA particles contain a number of organic compounds as well as a variable amount of liquid water, which has low  $T_g$  (136 K) and can act as a plasticizer (Mikhailov et al., 2009; Koop et al., 2011). Under humid conditions, SOA particles take up water by hygroscopic growth in response to RH, lowering  $T_g$  and viscosity of SOA particles.”*

Comment 12: Line 259: Another estimate, dependence of viscosity on temperature, requiring an estimate of the fragility constant, D. Sensitivity calcs are provided in Section 3 for the value of D, but no discussion of the accuracy of Eqns. 4 & 5 are presented. Giving the fragility parameter the symbol "D" is an unfortunate choice since diffusivity is usually represented by D as well, and isn't the diffusivity of molecules in aerosol particles the parameter that really matters, not the viscosity?

These equations are well established in the glass community as detailed in cited references (Angell, 1995, 1997). The symbol for fragility strength, D, is used by the glass community and we have chosen to maintain this convention. In our previous publications, we used 'D<sub>b</sub>' for bulk diffusivity. Please note that diffusivity estimations are beyond the scope of this study (see our response to the first comment).

Comment 13: Line 288: Please briefly discuss this more "profound meaning" of the Vogel temperature. There are a lot of concepts and terms used here that are not familiar to the atmospheric chemistry audience.

We have revised the manuscript to clarify this concept as follows:

*Line 288-295: “For the WLF equation,  $T_g$  is the reference temperature and there is a linear dependence assumed between temperature and free volume (O’Connell and McKenna, 1999; Huang and McKenna, 2001; Metatla and Soldera, 2007). For the VTF equation, the reference is the Vogel temperature ( $T_0$ )—a hypothetical temperature at which all non-vibrational motion ceases and viscosity becomes infinite and the theoretical foundation of the VTF equation includes both thermodynamic and kinetic considerations (O’Connell and McKenna, 1999; Huang and McKenna, 2001; Metatla and Soldera, 2007).”*

Comment 14-16: Line 305: There are highly relevant measurements of viscosity of SOA, or of its impacts (or lack thereof) on mixing timescales that are missing here, such as the papers by Ye, Gorkowski, and Liu mentioned above. Line 317: Up to what RH values is the viscosity of alpha-pinene SOA significant? My understanding of the literature is that above a rather low RH threshold of 20-30%. I think the importance of viscosity is again being overstated here, and again the mixing experiments are a better direct probe of how viscosity might affect vapor uptake and growth. This needs to be discussed more quantitatively than referring to "low RH". Sect. 3.2: Refer to the recent mixing experiments involving toluene by Ye et al. Fig. 10 would be much more meaningful if the estimated mixing/equilibration timescale was added to the right y-axis. Just plotting it as viscosity is not meaningful to most readers. The important effect is how viscosity affect

diffusivity, which determines equilibration timescales. You will need to discuss the important issues of converting between viscosity and diffusivity.

The goal of this section is to compare our viscosity estimation method with viscosity measurements—estimations of bulk diffusivity and mixing timescales are beyond the scope of this study. We also do not discuss the effects of viscosity on vapor uptake and particle growth. Equilibration timescale is not only a function of viscosity and bulk diffusivity, but it also depends strongly on other factors including accommodation coefficient, particle number concentration, and particle size (Shiraiwa and Seinfeld, 2012). Thus, even though we agree that equilibration timescales would be highly important, they are beyond the scope of this study. The suggested references are included in the introduction (see our response 1).

Comment 17: Line 307: "The wide range of viscosities reported for  $\alpha$ -pinene SOA may indicate that the O:C values may be different in different experiments." This frankly is quite sloppy. The average O:C value will change just with changes in aerosol mass concentration, as the less volatile components are typically more oxidized. And then there are all the important effects of using different chemical aging mechanisms to form the SOA. Not to mention the interesting effects of water vapor itself on the chemical composition of SOA. How is this accounted for? The plasticization effect of increased water vapor is important but it also changes the reaction products, as these authors recently reported: Hinks, M. L., Montoya-Aguilera, J., Ellison, L., Lin, P., Laskin, A., Laskin, J., Shiraiwa, M., Dabdub, D., and Nizkorodov, S. A.: Effect of relative humidity on the composition of secondary organic aerosol from the oxidation of toluene, *Atmos. Chem. Phys.*, 18, 1643-1652, <https://doi.org/10.5194/acp-18-1643-2018>, 2018.

Even though the O:C ratio can affect the phase state, the O:C ratio of SOA were unfortunately unavailable for most studies, with the exception of Zhang et al (2015) which reported O:C  $\approx$  0.46. We agree that RH upon SOA formation can affect chemical composition and phase of SOA particles (Kidd et al., 2014; Hinks et al., 2018). We have revised the manuscript to clarify this point as follows:

*Lines 307-314: "The wide range of experimentally measured viscosities reported for  $\alpha$ -pinene SOA, particularly from 30-60% RH is most likely a consequence of the different experimental approaches, mass loadings and O:C ratios for each experiment. For instance, Grayson et al. (2016) used mass loadings of 121 to 14000  $\mu\text{g m}^{-3}$  and observed that viscosity decreased as mass loading increased. Higher mass loadings would lead to greater partitioning of semi-volatile and lower molar mass compounds into the particle phase, which would lead to the decrease of  $T_g$  and viscosity of the resulting SOA mixture. They concluded that their results should be considered a lower limit for viscosity of  $\alpha$ -pinene SOA in the atmosphere."*

Comment 18: Line 351: The high sensitivity of predicted viscosity to  $T_g$  is really concerning considering that  $T_g$  is estimated from  $T_m$ , which is also estimated from the EPA EPI Suite model. The effect of varying  $D$  and  $\kappa$  is briefly discussed, but what is critically missing is an assessment of the accuracy and uncertainty in the predicted viscosity. When you consider how many steps are taken to calculate viscosity, and how



sensitive it is to  $T_g$ , I am left with little confidence in this model's predictions.

Please refer to response 9. Our  $T_g$  parameterization is developed from experimental  $T_g$  and the Boyer-Kauzmann rule using  $T_m$  is used only for comparison. Note that the  $T_g$  of isoprene and  $\alpha$ -pinene SOA used in Figs 4-6 are adopted from Table A1 in Berkemeier et al. (2014) who showed the  $T_g$  of isoprene and  $\alpha$ -pinene SOA varied with O:C. We did not use Eq. (1) or (2) to predict the  $T_g$  of isoprene and  $\alpha$ -pinene SOA here because elemental composition of SOA for different experiments was unavailable. Thus, the performance of viscosity predictions of isoprene and  $\alpha$ -pinene SOA shown in Figs 4-6 has no relation to Eq. (1) or (2). For viscosity predictions, VTF and WLF equations are established and validated in the glass community. In fact, these equations have also been widely used in the atmospheric community to predict the viscosity of SOA mixtures (Berkemeier et al., 2014; Wang et al., 2015; Schill et al., 2013; Maclean et al., 2017; Rothfuss and Petters, 2017a, 2017b; Pratap et al., 2018). Figure 4 in our manuscript shows that the VTF predictions assuming  $D$  of 10 agree well with the WLF predictions.

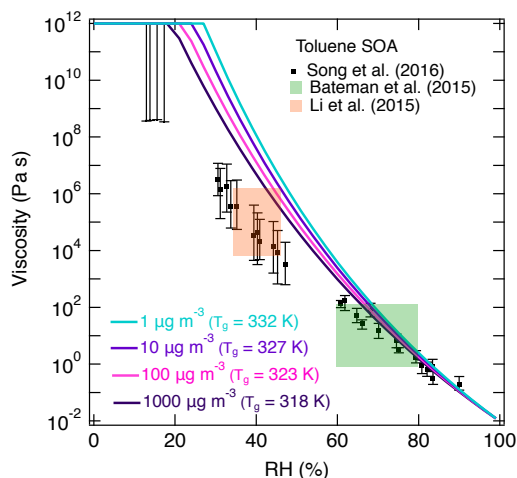
Comment 19: Line 329: See comment above for Line 307. The important roles of aerosol mass loading and other experimental conditions can be discussed in a much more meaningful and quantitative manner. We have a pretty good grasp of how the aerosol mass loading affects partitioning, volatility, O:C, and thus predicted viscosity, yet here it is presented as some nebulous unconstrained factor.

We agree that mass loading can affect viscosity, as it affects the chemical composition of SOA particles. Grayson et al. (2016) observed a decrease in  $\alpha$ -pinene SOA viscosity when mass loading increased, with a factor of 45 decrease in viscosity observed when mass loading increased from 121 to 14000  $\mu\text{g m}^{-3}$  at <0.5% RH. Song et al. (2016) investigated this effect for toluene SOA produced at two different mass loadings (60-100 and 600-1000  $\mu\text{g m}^{-3}$ ) and compared their results to previous studies on toluene SOA by Bateman et al. (2015) (30-50  $\mu\text{g m}^{-3}$ ) and Li et al. (2015) (44-125  $\mu\text{g m}^{-3}$ ). They did not observe a significant effect of mass loading on viscosity, concluding that toluene SOA mixtures are not very sensitive to mass loading effects.

To follow up on this issue, we carried out a sensitivity study of mass loadings on viscosity of toluene SOA using HR-MS data. The saturation mass concentration ( $C^0$ ) was predicted for each component using the molecular corridor approach (Li et al., 2016). Assuming that the mass signal intensity is proportional to the total mass of the compound in the mixture, and applying the absorptive partitioning theory (Pankow, 1994), particle-phase concentrations of each compounds were estimated at different mass loading values (1-1000  $\mu\text{g m}^{-3}$ ) followed by  $T_g$  and viscosity estimations for each mass loading using the scaled particle-phase concentrations. Mass loading effects on viscosity can be clearly observed in new Fig. A3: as mass loading increases, the glass transition temperature of the SOA mixture and the viscosity decrease. At low RH, the predicted viscosities span up to two orders of magnitude, while at high RH they have little difference. The mass loading effect is smaller than that observed when model parameters ( $T_{g,\text{org}}$ ,  $\kappa$ ,  $k_{\text{GT}}$  and  $D$ ) are varied and its overall effect is not large, which is consistent with Song et al. (2016). Mass loading effects may warrant further investigations with dedicated experiments

combined with modeling partitioning and viscosity predictions. We have added the following text to our manuscript:

Lines 1015-1021:



**“Figure A3.** Effect of mass loading on predicted viscosity for toluene SOA. Solid lines represent the predicted viscosity with Eq.(2) using chemical composition of toluene SOA formed at low RH. Viscosity was predicted with different mass loadings ranging from 1-1000  $\mu\text{g m}^{-3}$ . Markers and shaded boxes represent experimentally measured viscosity values. Song et al. (2016) mass loadings were 60-100 and 600-1000  $\mu\text{g m}^{-3}$ . Bateman et al., (2015) and Li et al., (2015) mass loadings were 30-50  $\mu\text{g m}^{-3}$  and 44-125  $\mu\text{g m}^{-3}$ , respectively.”

Lines 307-314: “The wide range of experimentally measured viscosities reported for  $\alpha$ -pinene SOA, particularly from 30-60% RH is most likely a consequence of the different experimental approaches, mass loadings and O:C ratios for each experiment. For instance, Grayson et al. (2016) used mass loadings of 121 to 14000  $\mu\text{g m}^{-3}$  and observed that viscosity decreased as mass loading increased. Higher mass loadings would lead to greater partitioning of semi-volatile and lower molar mass compounds into the particle phase, which would lead to the decrease of  $T_g$  and viscosity of the resulting SOA mixture. They concluded that their results should be considered a lower limit for viscosity of  $\alpha$ -pinene SOA in the atmosphere.”

Lines 447-460: “In addition, different mass loadings may have affected viscosity. Song et al. (2016) measured viscosity at two different mass loadings (60-100 and 600-1000  $\mu\text{g m}^{-3}$ ) and compared their results to Bateman et al. (2015) (30-50  $\mu\text{g m}^{-3}$ ) and Li et al. (2015) (44-125  $\mu\text{g m}^{-3}$ ), observing little impact of mass loadings on viscosity. We carried out a sensitivity study of mass loadings on viscosity using a set of compounds detected by HRMS. The saturation mass concentration was predicted for each component using the molecular corridor approach (Li et al., 2016). Assuming that the mass signal intensity is proportional to the total mass concentration of the compound in the mixture, and applying the absorptive partitioning theory (Pankow, 1994), particle-phase concentrations of each compound were predicted to estimate  $T_g$  at different organic aerosol mass loading values (1-1000  $\mu\text{g m}^{-3}$ ). The glass transition temperature of the

*SOA mixture decreases as mass loading increases. Viscosity decreases up to two orders of magnitude at low RH, while at high RH they have little difference as shown in Fig. A3. Simultaneous measurements of viscosity and chemical composition with different mass loadings should be performed in future studies.”*

Comment 20: Line 390: Analyte solubility in the solvent used is also an important factor in the detection efficiency using DESI.

We agree that the choice of solvent is an important factor for this characterization method. We selected the solvent to maximize solubility and ionization efficiency of OA compounds in ESI. For SOA, acetonitrile or methanol represent a good choice because they extract all of the organics from the sample and provide stable ESI conditions (Hinks et al., 2017).

Comment 21: Line 387: The key role of aerosol loadings is again treated very vaguely. What were the mass loadings for these two different experiments? The OFR method typically works at much much higher loadings than in a large smog chamber. Please be specific here. There is no need to treat the aerosol loading as some unknown factor.

The mass loadings for the experiment are listed at the beginning of the section. We have also added them to the caption for Figure 7 in the revised manuscript:

*Lines 974-975, Figure 7 caption: “Mass loadings were  $23 \mu\text{g m}^{-3}$  for LRH and  $8 \mu\text{g m}^{-3}$  for HRH (Hinks et al., 2017).“*

Comment 22: Sect. 3.3: The analysis of biomass burning particles, while valiant, is really unsatisfying. First, why weren't experiments on BBA when AMS data is available to provide elemental analysis used? Surely there must be experiments on BBA where AMS and the other necessary measurements were made? If not I suggest this entire section be omitted, as the results are terrible, because the input data from the experiments does not properly constrain the model. The exclusion of CHOS and CHON compounds from the model is a problem for BBA, where organonitrates are common components, and organosulfates can be as well. It seems that applying the model to BBA is too premature. The authors could move this to the SI if they think there is some value in the exercise.

The point of our analysis is to compare the predicted viscosity with HRMS data using two different ionization methods. Our intention was not to provide accurate estimates of viscosity of BBA especially since, as the referee also pointed out, we do not currently have equations to predict  $T_g$  for N and S containing compounds. The value of Section 3.3 is enabling a comparison of data from the ESI and APPI methods to discuss the variability in the modeling prediction. For this reason, we opted to include this section in the main manuscript. To clarify this point we added the following text:

*Lines 478-480: “Please note that we do not intend to provide accurate estimates of ambient biomass burning particles (as inorganic components are also not included in this analysis), but we investigate how the use of different ionization methods would lead to*

*variations in our viscosity predictions.”*

Comment 23: Line 531: "Current T<sub>g</sub> parameterizations do not consider functionality or molecular structure explicitly and further measurements of T<sub>g</sub> and viscosity of SOA would allow us to refine the method presented in this study." This is precisely why the functional group-based approach of Rothfuss and Petters is vastly superior than the T<sub>g</sub> based approach here, and yet this closely related alternate model is barely discussed here. As mentioned earlier, in the end you get an estimate of viscosity (following a series of steps with their own uncertainties), but the property that really matters is diffusivity, and unfortunately the Stokes-Einstein relationship between viscosity and diffusivity is inaccurate by more than one order of magnitude in high viscosity systems (Marshall et al., 2016). So it is not clear to me what this rather simplistic estimate of viscosity from T<sub>g</sub> really tells us about important aerosol physicochemical properties in the end.

As we mentioned in the above responses, Rothfuss and Petters (2017) did not provide a method to predict viscosity of complex multi-component SOA mixtures. Diffusivity estimations are beyond the scope of this study and will be investigated in future studies (please see response 1).

Comment 24: As Referee 2 pointed out, there is little data > 500 g/mol plotted in Fig 3a to fit to.

Please see our response to Referee 2.

Comment 25: Fig. 4a: The slope of the experimental data is quite different from the predicted lines. Please discuss as this is concerning. The experimental data has a much shallower slope. A similar discrepancy is seen in Fig. 5. These issues give me even less confidence in the model.

As illustrated in Figures 5(d) and 6(d), the slope of the curve decreases at low RH if the values of  $k_{GT}$  or  $\kappa$  are lower at 1.0 or 0.05, respectively. However, the curve does not fit well at high RH with this value of  $k_{GT}$ . Available experiments indicate that  $k_{GT}$  should be around 2-3 (Dette et al., 2014; Dette and Koop, 2015). We acknowledge that our method has certain limits, which need to be investigated further.

#### **References:**

- Angell, C. A.: Formation of glasses from liquids and biopolymers, *Science*, 267, 1924-1935, 1995.
- Angell, C. A.: Entropy and fragility in supercooling liquids, National Institute of Standards and Technology, *Journal of Research*, 102, 171-185, 1997.
- Bateman, A. P., Belassein, H., and Martin, S. T.: Impactor Apparatus for the Study of Particle Rebound: Relative Humidity and Capillary Forces, *Aerosol Sci. Technol.*, 48, 42-52, 2014.

Bateman, A. P., Bertram, A. K., and Martin, S. T.: Hygroscopic Influence on the Semisolid-to-Liquid Transition of Secondary Organic Materials, *J. Phys. Chem. A*, 119, 4386-4395, 2015.

Booth, A. M., Murphy, B., Riipinen, I., Percival, C. J., and Topping, D. O.: Connecting Bulk Viscosity Measurements to Kinetic Limitations on Attaining Equilibrium for a Model Aerosol Composition, *Environ. Sci. Technol.*, 48, 9298-9305, 2014.

Cappa, C. D., and Wilson, K. R.: Evolution of organic aerosol mass spectra upon heating: implications for OA phase and partitioning behavior, *Atmos. Chem. Phys.*, 11, 1895-1911, 2011.

Cappa, C. D., and Wilson, K. R.: Multi-generation gas-phase oxidation, equilibrium partitioning, and the formation and evolution of secondary organic aerosol, *Atmos. Chem. Phys.*, 12, 9505-9528, 2012.

Charnawskas, J. C., Alpert, P. A., Lambe, A., et al.: Condensed-phase biogenic-anthropogenic interactions with implications for cold cloud formation, *Faraday Discuss.*, 200, 165-194, 2017.

Chenyakin, Y., Ullmann, D. A., Evoy, E., Renbaum-Wolff, L., Kamal, S., and Bertram, A. K.: Diffusion coefficients of organic molecules in sucrose–water solutions and comparison with Stokes–Einstein predictions, *Atmos. Chem. Phys.*, 17, 2423-2435, 2017.

Detle, H. P., Qi, M., Schröder, D. C., Godt, A., and Koop, T.: Glass-forming properties of 3-Methylbutane-1,2,3-tricarboxylic acid and its mixtures with water and pinonic acid, *J. Phys. Chem. A*, 118, 7024-7033, 2014.

Detle, H. P., and Koop, T.: Glass Formation Processes in Mixed Inorganic/Organic Aerosol Particles, *J. Phys. Chem. A*, 119, 4552-4561, 2015.

Gorkowski, K., Donahue, N. M., and Sullivan, R. C.: Emulsified and Liquid–Liquid Phase-Separated States of  $\alpha$ -Pinene Secondary Organic Aerosol Determined Using Aerosol Optical Tweezers, *Environ. Sci. Technol.*, 51, 12154-12163, 2017.

Hinks, M. L., Montoya-Aguilera, J., Ellison, L., Lin, P., Laskin, A., Laskin, J., Shiraiwa, M., Dabdub, D., and Nizkorodov, S. A.: Effect of relative humidity on the composition of secondary organic aerosol from the oxidation of toluene, *Atmos. Chem. Phys.*, 18, 1643-1652, 2018.

Ignatius, K., Kristensen, T. B., Järvinen, E., et al.: Heterogeneous ice nucleation of viscous secondary organic aerosol produced from ozonolysis of  $\alpha$ -pinene, *Atmos. Chem. Phys.*, 16, 6495-6509, 2016.

Jathar, S. H., Cappa, C. D., Wexler, A. S., Seinfeld, J. H., and Kleeman, M. J.: Multi-generational oxidation model to simulate secondary organic aerosol in a 3-D air quality model, *Geosci. Model Dev.*, 8, 2553-2567, 2015.

Kidd, C., Perraud, V., Wingen, L. M., and Finlayson-Pitts, B. J.: Integrating phase and composition of secondary organic aerosol from the ozonolysis of alpha-pinene, *Proc. Natl. Acad. Sci. U.S.A.*, 111, 7552-7557, 2014.

Knopf, D. A., Alpert, P. A., and Wang, B.: The Role of Organic Aerosol in Atmospheric Ice Nucleation: A Review, *ACS Earth and Space Chemistry*, 2018.

Koop, T., Bookhold, J., Shiraiwa, M., and Pöschl, U.: Glass transition and phase state of organic compounds: dependency on molecular properties and implications for secondary organic aerosols in the atmosphere, *Phys. Chem. Chem. Phys.*, 13, 19238-19255, 2011.

Li, Y., Pöschl, U., and Shiraiwa, M.: Molecular corridors and parameterizations of volatility in the chemical evolution of organic aerosols, *Atmos. Chem. Phys.*, 16, 3327-3344, 2016.

Liu, P., Li, Y. J., Wang, Y., Gilles, M. K., Zaveri, R. A., Bertram, A. K., and Martin, S. T.: Lability of secondary organic particulate matter, *Proc. Natl. Acad. Sci. U.S.A.*, 113, 12643-12648, 2016.

Loza, C. L., Coggon, M. M., Nguyen, T. B., Zuend, A., Flagan, R. C., and Seinfeld, J. H.: On the mixing and evaporation of secondary organic aerosol components, *Environ. Sci. Technol.*, 47, 6173-6180, 2013.

Mai, H., Shiraiwa, M., Flagan, R. C., and Seinfeld, J. H.: Under What Conditions Can Equilibrium Gas-Particle Partitioning Be Expected to Hold in the Atmosphere?, *Environ. Sci. Technol.*, 49, 11485-11491, 2015.

Mikhailov, E., Vlasenko, S., Martin, S. T., Koop, T., and Pöschl, U.: Amorphous and crystalline aerosol particles interacting with water vapor: conceptual framework and experimental evidence for restructuring, phase transitions and kinetic limitations, *Atmos. Chem. Phys.*, 9, 9491-9522, 2009.

Murray, B. J., Wilson, T. W., Dobbie, S., et al.: Heterogeneous nucleation of ice particles on glassy aerosols under cirrus conditions, *Nat. Geosci.*, 3, 233-237, 2010.

Nakanishi, M., and Nozaki, R.: Systematic study of the glass transition in polyhydric alcohols, *Physical Review E*, 83, 051503, 2011.

Pankow, J. F.: An absorption model of gas-particle partitioning of organic-compounds in the atmosphere, *Atmos. Environ.*, 28, 185-188, 1994.

Perraud, V., Bruns, E. A., Ezell, M. J., et al.: Nonequilibrium atmospheric secondary organic aerosol formation and growth, *Proc. Natl. Acad. Sci. U.S.A.*, 109, 2836-2841, 2012.

Roldin, P., Eriksson, A. C., Nordin, E. Z., et al.: Modelling non-equilibrium secondary organic aerosol formation and evaporation with the aerosol dynamics, gas- and particle-phase chemistry kinetic multilayer model ADCHAM, *Atmos. Chem. Phys.*, 14, 7953-7993, 2014.

Rothfuss, N. E., and Petters, M. D.: Influence of Functional Groups on the Viscosity of Organic Aerosol, *Environ. Sci. Technol.*, 51, 271-279, 2017.

Sastri, S. R. S., and Rao, K. K.: A new group contribution method for predicting viscosity of organic liquids, *The Chemical Engineering Journal*, 50, 9-25, 1992.

Schill, G. P., De Haan, D. O., and Tolbert, M. A.: Heterogeneous Ice Nucleation on Simulated Secondary Organic Aerosol, *Environ. Sci. Technol.*, 48, 1675-1682, 2014.

Shiraiwa, M., and Seinfeld, J. H.: Equilibration timescale of atmospheric secondary organic aerosol partitioning, *Geophys. Res. Lett.*, 39, L24801, 2012.

- Shiraiwa, M., Yee, L. D., Schilling, K. A., Loza, C. L., Craven, J. S., Zuend, A., Ziemann, P. J., and Seinfeld, J. H.: Size distribution dynamics reveal particle-phase chemistry in organic aerosol formation, *Proc. Natl. Acad. Sci. U.S.A.*, 110, 11746-11750, 2013.
- Vaden, T. D., Imre, D., Beranek, J., Shrivastava, M., and Zelenyuk, A.: Evaporation kinetics and phase of laboratory and ambient secondary organic aerosol, *Proc. Natl. Acad. Sci. U.S.A.*, 108, 2190-2195, 2011.
- van der Sman, R. G. M.: Predictions of Glass Transition Temperature for Hydrogen Bonding Biomaterials, *J. Phys. Chem. B*, 117, 16303-16313, 2013.
- Wang, B. B., Lambe, A. T., Massoli, P., Onasch, T. B., Davidovits, P., Worsnop, D. R., and Knopf, D. A.: The deposition ice nucleation and immersion freezing potential of amorphous secondary organic aerosol: Pathways for ice and mixed-phase cloud formation, *J. Geophys. Res.-Atmos.*, 117, D16209, 2012a.
- Wang, B. B., Laskin, A., Roedel, T., Gilles, M. K., Moffet, R. C., Tivanski, A. V., and Knopf, D. A.: Heterogeneous ice nucleation and water uptake by field-collected atmospheric particles below 273 K, *J. Geophys. Res.-Atmos.*, 117, D00v19, 2012b.
- White, R. P., and Lipson, J. E. G.: Polymer Free Volume and Its Connection to the Glass Transition, *Macromolecules (Washington, DC, U. S.)*, 49, 3987-4007, 2016.
- Ye, Q., Robinson, E. S., Ding, X., Ye, P., Sullivan, R. C., and Donahue, N. M.: Mixing of secondary organic aerosols versus relative humidity, *Proc. Natl. Acad. Sci. U.S.A.*, 113, 12649-12654, 2016.
- Ye, Q., Upshur, M. A., Robinson, E. S., Geiger, F. M., Sullivan, R. C., Thomson, R. J., and Donahue, N. M.: Following Particle-Particle Mixing in Atmospheric Secondary Organic Aerosols by Using Isotopically Labeled Terpenes, *Chem*, 4, 318-333, 2018.
- Yli-Juuti, T., Pajunoja, A., Tikkanen, O.-P., et al.: Factors controlling the evaporation of secondary organic aerosol from  $\alpha$ -pinene ozonolysis, *Geophys. Res. Lett.*, 44, 2562-2570, 2017.
- Zaveri, R. A., Easter, R. C., Shilling, J. E., and Seinfeld, J. H.: Modeling kinetic partitioning of secondary organic aerosol and size distribution dynamics: representing effects of volatility, phase state, and particle-phase reaction, *Atmos. Chem. Phys.*, 14, 5153-5181, 2014.
- Zaveri, R. A., Shilling, J. E., Zelenyuk, A., et al.: Growth Kinetics and Size Distribution Dynamics of Viscous Secondary Organic Aerosol, *Environ. Sci. Technol.*, 52, 1191-1199, 2018.

## Response to the comments of Anonymous Referee #2

(Referee comments in black, our responses in blue)

Referee General Comment:

This ACPD article describes a modeling method to estimate the glass transition temperature and viscosity of organic mixtures and secondary organic aerosols (SOA) with molecular weight up to 1100 g mol<sup>-1</sup>. This work continues the work that the authors published before, but the difference is that previous work can only predict organics with molar masses up to 450 g mol<sup>-1</sup> while this work extends the molar mass region twice as much as the previous work. The scientific significance of this study is that the current model is able to predict the glass transition temperatures and viscosities of oligomers instead of just small organic molecules, which can be applied those oligomer-rich SOA systems. I like that even though the paper focus on molecular mass > 450 g/mol, the fitting equation still fit for molecular < 450 g/mol, and the results are even better. This study describes the modeling process, and then utilizes experimental data to verify the model. The experimental data add credibility to the modeling results. Overall, the manuscript is sound and after addressing the following issues, it is suitable to be published on ACP.

Responses:

We thank Anonymous Referee #2 for the review and the positive evaluation of our manuscript. Based on your constructive suggestions for improvement, we will expand discussions in the revised manuscript as detailed below.

In Figure 1, it looks like there are only 8 compounds whose molar masses are larger than 450 g/mol, which is quite few compared with the number of compounds whose molar masses are below 450 g/mol. Would the limited number of compounds with higher molar masses causing a skew when modeling their viscosity and glass transition temperatures?

We share this concern as well. As pointed out in the manuscript, there are only eight experimental data points available on the glass transition temperatures of higher molar mass compounds ( $M > 450 \text{ g mol}^{-1}$ ) of atmospheric relevance, as compiled by Rothfuss and Petters. Including this dataset has enabled us to extend the molar mass range to which our method applies. We have been reviewing polymer data for glass transition values, but have found that the molar mass is often ill-defined for polymer distributions in these studies, making it hard to be incorporated in our method. We plan to continue to refine our method as additional glass transition data on high molar mass compounds becomes available. We have added the following sentences in the revised manuscript:

*Lines 137-138: "Eight of these compounds are carbohydrates with  $M > 450 \text{ g mol}^{-1}$ ."*

*Lines 179-180: "We plan to continue to refine our method as additional glass transition data on high molar mass compounds become available."*



In Figure 4 (a), the author uses measured viscosity data of alpha-pinene SOA to model the viscosity trend with RH. The author seems to heavily rely on the data from Renbaum-Wolff because that set of data covers a wider RH. However, in Renbaum- Wolff et al. specified that their data was only the water-soluble part of SOA, while all the other measured data listed in the plot were based on the whole SOA. The model does not seem to distinguish these two differences and mix all the data together. Wouldn't this approach lead to inaccuracy to predict the viscosity of total SOA? Maybe it is better for the author to use the measured viscosity of total SOA to predict SOA's viscosity, and leave the water-soluble part of the SOA to another plot and estimate its viscosity individually.

Our viscosity predictions are based on four parameters (glass transition temperature of dry SOA mixture ( $T_{g,dry}$ ), hygroscopicity ( $\kappa$ ), fragility and Gordon-Taylor constant ( $k_{GT}$ ). Especially  $T_{g,dry}$  and  $\kappa$  may be different for water-soluble or total SOA. Moreover, different studies generated SOA in different conditions (e.g., flow tube vs. chamber, different oxidant concentrations, etc.) that would lead to variations in these parameters. While we agree that this approach would lead to inaccuracy/uncertainties in comparing our predictions with different experiments, there are insufficient data points to have separate panels. In accordance with your comment, we clarify this point in the revised manuscript as shown below and also make data points by Renbaum-Wolff in open markers in Fig. 4 and 5 to make it clear that these data points are for water-soluble components.

*Lines 314-316: "It should also be noted that the viscosity measurements from Renbaum-Wolff et al. (2013) were for the water-soluble portion of the SOA."*

*Lines 944-945, added to caption for Figure 4: "Panel (a): Renbaum-Wolff et al. (2013) data represents viscosity for water-soluble portion of SOA;"*

Figure 4(b) was based on Song et al. 2015 data and Bateman et al. 2015 data. I checked Song et al. 2015 and found out that their data was based on SOA condensation from the potential aerosol mass (PAM) reactor (Song, Liu et al. 2015). In the ambient environment, it has shown that the majority of the isoprene SOA is formed by heterogeneous reactions with the acidic sulfate particles, rather than condensation of semi-volatile species (Lin, Zhang et al. 2013, Surratt, Chan et al. 2010). Heterogeneous reactions of isoprene products will be able to form more oligomers and lead to a lower viscosity (Gaston, Riedel et al. 2014). Therefore the experimental data from Figure 4(b) may not represent the ambient isoprene SOA viscosity. At the very least the author should make it clear in the manuscript (both Figure 4(b) and Figure 10) about the limitation of this study so more motivation is put for others to perform experimental viscosity measurement

on ambient-like isoprene SOA particles generated from heterogeneous reactions.

Thank you for this insightful comment. We agree that laboratory-generated SOA may be different from ambient SOA. Following your comment, we have added the following discussion in the revised manuscript:

*Lines 333-342: “In contrast to  $\alpha$ -pinene SOA, there are limited viscosity measurements for isoprene SOA. While the predicted viscosity is consistent with the experimental data, comparison of our model predictions to additional measurements is strongly recommended. Song et al. (2015) prepared their samples in a potential aerosol mass (PAM) reactor while those investigated by Bateman et al. (2015) were generated in a smog chamber. It has been suggested that under ambient conditions the majority of isoprene-derived SOA can be derived through heterogeneous interactions with acidic sulfate particles forming oligomers (Lin et al., 2013; Surratt et al., 2010)(Gaston et al., 2014), which may increase viscosity. Further studies are warranted to compare laboratory-generated and ambient isoprene SOA, and to investigate the effect of the acidic seed on the viscosity.”*

In Figure 9 and 10, the author used ESI and APPI data to model the viscosity value of biomass burning aerosols. Biomass burning aerosols typically also contain inorganic components as well but the author neglects that part and only take the organic component into consideration. How would the inorganic components affect the viscosity of the total aerosols? Maybe the author should be a bit more specific when they mention biomass burning particles?

Please note that we do not intend to provide accurate estimates of ambient biomass burning particles in this study, but we investigate how the use of different ionization methods would lead to variations in our viscosity predictions. If the particles are well-mixed with the inorganic fraction (such as sulfate and nitrate, which have with lower  $T_g$ ), that would lead to decrease of viscosity (Dette and Koop, 2015). A liquid-liquid phase separation is most likely to occur when the O:C ratio of the organic fraction is below 0.5 (You et al., 2014) and in this case the predicted viscosity would only apply to the organic phase. We have added the following text to Section 3.3:

*Lines 478-480: “Please note that we do not intend to provide accurate estimates of ambient biomass burning particles (as inorganic components are also not included in this analysis), but we investigate how the use of different ionization methods would lead to variations in our viscosity predictions.”*

Editorial comments:

Lines 135-137: When the author says: ” Specifically, data for 76 aliphatic alcohols, 39

carbohydrates and their derivatives...”, do all these compounds have molar masses larger than 450 g/mol? It sounds like it because the way the author phrase the sentence. If not, the author may want to revise this sentence to make it more clear and indicate which compounds have molar masses  $> 450$ .

Thank you for this key comment. The eight compounds with  $M > 450 \text{ g mol}^{-1}$  are all carbohydrates (Fig. 4 in Rothfuss and Petters, 2017). This could lead to a skew when applying our parameterization in high molar mass compounds containing multifunctional groups. We will continue to refine our method as additional glass transition data on high molar mass compounds becomes available, especially the compounds containing multifunctional groups. The following statement has been added to this section:

*Lines 137-138: “Eight of these compounds are carbohydrates with  $M > 450 \text{ g mol}^{-1}$ .”*

Table 1, nc(0) symbol is not centered in the table;

Symbol has been centered in its column.

Line 903, the parenthesis after 2014 is missing;

This was corrected.

Line 909, the letters are partially overlapping with the table.

This was fixed.

1 **Predicting the glass transition temperature and viscosity of secondary**  
2 **organic material using molecular composition**

3

4

5 **Wing-Sy Wong DeRieux<sup>1§</sup>, Ying Li<sup>1§</sup>, Peng Lin<sup>2</sup>, Julia Laskin<sup>2</sup>, Alexander Laskin<sup>2</sup>,**  
6 **Allan K. Bertram<sup>3</sup>, Sergey A. Nizkorodov<sup>1</sup>, and Manabu Shiraiwa<sup>1\*</sup>**

7

8 [1] Department of Chemistry, University of California, Irvine, CA 92697-2025, USA

9 [2] Department of Chemistry, Purdue University, West Lafayette, IN 47907-2084, USA

10 [3] Department of Chemistry, University of British Columbia, Vancouver, BC V6T 1Z1, Canada

11

12 § These authors contributed equally to this work.

13 \*Correspondence to: M. Shiraiwa (m.shiraiwa@uci.edu)

14

15 *Submitted to Atmospheric Chemistry and Physics (ACP)*

16

17 **Abstract:**

18 Secondary organic aerosols (SOA) account for a large fraction of submicron particles in the  
19 atmosphere. SOA can occur in amorphous solid or semi-solid phase states depending on  
20 chemical composition, relative humidity (RH), and temperature. The phase transition between  
21 amorphous solid and semi-solid states occurs at the glass transition temperature ( $T_g$ ). We have  
22 recently developed a method to estimate  $T_g$  of pure compounds containing carbon, hydrogen, and  
23 oxygen atoms (CHO compounds) with molar mass less than 450 g mol<sup>-1</sup> based on their molar  
24 mass and atomic O:C ratio. In this study, we refine and extend this method for CH and CHO  
25 compounds with molar mass up to ~1100 g mol<sup>-1</sup> using the number of carbon, hydrogen, and  
26 oxygen atoms. We predict viscosity from the  $T_g$ -scaled Arrhenius plot of fragility (viscosity vs.  
27  $T_g/T$ ) as a function of the fragility parameter  $D$ . We compiled  $D$  values of organic compounds  
28 from literature, and found that  $D$  approaches a lower limit of ~10 (+/- 1.7) as the molar mass  
29 increases. We estimated viscosity of  $\alpha$ -pinene and isoprene SOA as a function of RH by  
30 accounting for hygroscopic growth of SOA and applying the Gordon-Taylor mixing rule,  
31 reproducing previously published experimental measurements very well. Sensitivity studies were  
32 conducted to evaluate impacts of  $T_g$ ,  $D$ , hygroscopicity parameter ( $\kappa$ ), and the Gordon-Taylor  
33 constant on viscosity predictions. Viscosity of toluene SOA was predicted using the elemental  
34 composition obtained by high-resolution mass spectrometry (HRMS), resulting in a good  
35 agreement with the measured viscosity. We also estimated viscosity of biomass burning particles  
36 using the chemical composition measured by HRMS with two different ionization techniques:  
37 electrospray ionization (ESI) and atmospheric pressure photoionization (APPI). Due to  
38 differences in detected organic compounds and signal intensity, predicted viscosities at low RH  
39 based on ESI and APPI measurements differ by 2-5 orders of magnitude. Complementary

40 measurements of viscosity and chemical composition are desired to further constrain RH-  
41 dependent viscosity in future studies.

42

## 43 **1. Introduction**

44 Secondary organic aerosols (SOA) account for a large fraction of submicron particles in the  
45 atmosphere and they play an important role in climate, air quality and public health (Goldstein  
46 and Galbally, 2007; Jimenez et al., 2009). Traditionally, SOA particles were assumed to be  
47 liquid with dynamic viscosity  $\eta$  below  $10^2$  Pa s, but a number of recent studies have shown that  
48 they can also adopt amorphous semi-solid ( $10^2 \leq \eta \leq 10^{12}$  Pa s), or glassy solid ( $\eta > 10^{12}$  Pa s)  
49 states, depending on chemical composition and temperature (Zobrist et al., 2008; Koop et al.,  
50 2011; Huang et al., 2018; Reid et al., 2018). The phase state is also strongly affected by relative  
51 humidity, as water can act as a plasticizer to lower viscosity (Mikhailov et al., 2009). Ambient  
52 and laboratory-generated SOA particles have been observed to bounce off the smooth hard  
53 surface of an inertial impactor at low RH, implying a non-liquid state (Virtanen et al., 2010;  
54 Saukko et al., 2012; Bateman et al., 2015; Jain and Petrucci, 2015), whereas predominantly  
55 biogenic SOA particles in the Amazon basin did not bounce off the impactor surface at high RH,  
56 implying they are primarily liquid (Bateman et al., 2016). Upon dilution or heating, SOA  
57 particles were observed to evaporate unexpectedly slowly (Cappa and Wilson, 2011; Vaden et  
58 al., 2011), and recent modeling studies have evaluated the contributions of low diffusivity and  
59 volatility to slow evaporation rates (Roldin et al., 2014; Yli-Juuti et al., 2017). Measurements of  
60 viscosity of SOA bulk material derived from oxidation of  $\alpha$ -pinene (Renbaum-Wolff et al., 2013;  
61 Zhang et al., 2015; Hosny et al., 2016), limonene (Hinks et al., 2016), isoprene (Song et al.,

62 2015), and toluene (Song et al., 2016a) have confirmed that SOA particles adopt a wide range of  
63 viscosities.

64 The particle phase state has been shown to affect gas uptake and chemical transformation of  
65 organic compounds due to kinetic limitations of bulk diffusion (Shiraiwa et al., 2011; Abbatt et  
66 al., 2012; Kuwata and Martin, 2012; Zhou et al., 2013; Slade and Knopf, 2014; Arangio et al.,  
67 2015; Davies and Wilson, 2015; Wang et al., 2015; Berkemeier et al., 2016; Marshall et al.,  
68 2016; Liu et al., 2018; Pratap et al., 2018; Zhang et al., 2018). Molecular motion can be hindered  
69 in a highly viscous matrix, slowing down photochemical reactions in particles (Lignell et al.,  
70 2014; Hinks et al., 2016). Water diffusion can be still fast even in an amorphous solid matrix  
71 under room temperature, but it can be hindered significantly under low temperatures (Mikhailov  
72 et al., 2009; Zobrist et al., 2011; Bones et al., 2012; Berkemeier et al., 2014; Price et al., 2014),  
73 affecting homogeneous vs. heterogeneous ice nucleation pathways (Murray et al., 2010; Wang et  
74 al., 2012a; Wang et al., 2012b; Baustian et al., 2013; Schill and Tolbert, 2013; Berkemeier et al.,  
75 2014; Schill et al., 2014; Lienhard et al., 2015; Ignatius et al., 2016; Knopf et al., 2018). Despite  
76 the substantial implications of the SOA particle phase state, its effects on gas-particle  
77 interactions have not yet been considered explicitly in current climate and air quality models  
78 (Shrivastava et al., 2017).

79 Partitioning of semi-volatile compounds into viscous particles may result in kinetically-  
80 limited growth in contrast to quasi-equilibrium growth (Perraud et al., 2012; Shiraiwa and  
81 Seinfeld, 2012; Booth et al., 2014; Zaveri et al., 2014; Mai et al., 2015; Liu et al., 2016), which  
82 also affects the evolution of particle size distribution upon SOA growth (Shiraiwa et al., 2013;  
83 Zaveri et al., 2018). Chamber experiments probing mixing timescales of SOA particles derived  
84 by oxidation of various precursors such as isoprene, terpene, and toluene have observed strong

85 kinetic limitations at low RH, but not at moderate and high RH (Loza et al., 2013; Ye et al.,  
86 2016; Ye et al., 2018). Gorkowski et al. (2017) did not observe significant diffusion limitations  
87 for glycerol and squalene in  $\alpha$ -pinene SOA. Quasi-equilibrium versus kinetically-limited or non-  
88 equilibrium SOA growth remains an open issue and warrants further investigations.

89 Group contribution methods have been used to predict the viscosities of pure compounds  
90 when the functionality and molecular structure are known (Sastri and Rao, 1992; Rothfuss and  
91 Petters, 2017). Song et al. (2016) showed that estimations from group contribution approaches  
92 combined with either nonideal or ideal mixing reproduced the RH-dependent trends particularly  
93 well for the alcohol, di-, and tricarboxylic acid systems with viscosity of up to  $10^4$  Pa s. By  
94 contrast, model calculations overestimated the viscosity of more viscous compounds including  
95 mono-, di-, and trisaccharides by many orders of magnitude (Song et al., 2016b). A recent study  
96 compiled viscosity of organic compounds with atmospherically relevant functional groups,  
97 investigating the influence of the number and location of functional groups on viscosity  
98 (Rothfuss and Petters, 2017). *These studies provide important insights in estimating the viscosity  
99 of individual organic compounds.*

100 Particle phase state can be characterized by a glass transition temperature ( $T_g$ ), which is a  
101 characteristic temperature representing a non-equilibrium phase transition from a glassy solid  
102 state to a semi-solid state as the temperature increases (Koop et al., 2011). Recently, we have  
103 developed a method to estimate  $T_g$  of pure organic compounds comprised of carbon, hydrogen,  
104 and oxygen (CHO compounds) with molar mass less than  $450 \text{ g mol}^{-1}$  based on their molar mass  
105 and atomic O:C ratio (Shiraiwa et al., 2017). It has been applied successfully in a global  
106 chemistry climate model to predict  $T_g$  and the phase state of atmospheric SOA, which indicated  
107 that SOA particles are mostly liquid or semi-solid in the planetary boundary layer, while they



108 should be glassy in the middle and upper troposphere (Shiraiwa et al., 2017). A recent study  
109 provided a consistent result, suggesting that mixing timescales of organic molecules within SOA  
110 are often  $< 1$  h in a global planetary boundary layer (Maclean et al., 2017).

111 It has been shown that SOA particles contain oligomeric compounds with molar masses  
112 higher than  $450 \text{ g mol}^{-1}$  (Gao et al., 2004; Tolocka et al., 2004; Nizkorodov et al., 2011; Nozière  
113 et al., 2015), which makes the previously developed parameterization incomplete. In this study,  
114 we extend the parameterization of  $T_g$  to higher molar mass compounds, and apply it to high-  
115 resolution mass spectrometry data for toluene SOA and biomass burning particles. The  
116 Arrhenius approach and the Gordon-Taylor mixing rules were applied to estimate viscosity of  
117 SOA bulk materials to compare with the literature reported viscosity measurements. This method  
118 will be useful for estimations of viscosity of organic particles, for which high-resolution mass  
119 spectra are available. It can also be applied in global or regional models to evaluate impacts of  
120 the particle phase state on the role of SOA in climate and air quality.

121

## 122 **2. Parameterization development**

### 123 **2.1 Glass transition temperature**

124 Figure 1a shows the dependence of  $T_g$  on the molar mass ( $M$ ) of organic compounds. Solid  
125 markers represent measured  $T_g$  of 258 CHO compounds (Koop et al., 2011; Dette et al., 2014;  
126 Rothfuss and Petters, 2017), while open markers represent 654 CHO compounds in SOA  
127 (Shiraiwa et al., 2014). Markers are color-coded by atomic O:C ratio. Their melting points ( $T_m$ )  
128 were estimated by the Estimation Programs Interface (EPI) Suite software version 4.1 (US-EPA,  
129 2012) and their  $T_g$  were estimated using the Boyer-Kauzmann rule:  $T_g = g \cdot T_m$  with  $g = 0.7$  (Koop  
130 et al., 2011; Shiraiwa et al., 2017). [This rule can provide good estimates of  \$T\_g\$ , as has been](#)

131 validated in previous work (Koop et al., 2011) and also shown in Fig. A2(a). A subset of data  
132 shown in Figure 1 was originally published in Shiraiwa et al. (2017) for compounds with  $M <$   
133  $450 \text{ g mol}^{-1}$ . This version of the figure has been updated to include a number of experimentally  
134 measured  $T_g$  values of larger compounds with  $M$  up to  $1153 \text{ g mol}^{-1}$ , including aliphatic  
135 compounds containing OH and/or COOH groups. Specifically, data for 76 aliphatic alcohols, 39  
136 carbohydrates and their derivatives, 4 carboxylic acids, and 4 hydroxy acids, as compiled by  
137 Rothfuss and Petters (2017), have been added to Figure 1. Eight of these compounds are  
138 carbohydrates with  $M > 450 \text{ g mol}^{-1}$ . These updates are critical for reliable parameterization of  $T_g$   
139 based on  $M$ . When  $M$  increases above  $\sim 500 \text{ g mol}^{-1}$ , the slope of  $T_g$  decreases, making it  
140 challenging to extrapolate the low- $M$  data from the original Shiraiwa et al. (2017) study to higher  
141  $M$  values. When  $M$  increases to  $\sim 1000 \text{ g mol}^{-1}$ , the corresponding  $T_g$  appears to level at around  
142 420 K.

143 Such dependence on  $M$  has been described for polymers with the Fox-Flory equation:  
144  $T_g(M) = T_{g,\infty} - \frac{K_m}{M}$  (Fox Jr and Flory, 1950), where  $K_m$  is a constant and  $T_{g,\infty}$  is the asymptotic  
145 value of  $T_g$  specific to the polymer. We conducted a literature search and found that most of the  
146 reported  $T_{g,\infty}$  values fell below  $\sim 500 \text{ K}$  (Fox Jr and Flory, 1950; Onder et al., 1972; Montserrat  
147 and Colomer, 1984; Polymer handbook, 1999; Papadopoulos et al., 2004; Matsushima et al.,  
148 2017). The Fox-Flory equation works very well for high molar mass compounds and is also  
149 generally applicable to smaller compounds (Koop et al., 2011), as supported by an approximately  
150 linear dependence of  $T_g$  on the inverse molar mass in Fig. A1(a). Figure 1b plots the values of  $T_g$   
151 as a function of the atomic O:C ratio of organic molecules. Figures 1a and 1b clearly  
152 demonstrate that  $T_g$  depends primarily on the molar mass with a weak dependence on the atomic  
153 O:C ratio.

154 A parameterization for  $T_g$  calculation based on the molar mass and atomic O:C ratio was  
155 developed in our recent work, which is applicable to CH and CHO compounds with  $M < 450$  g  
156  $\text{mol}^{-1}$  (Shiraiwa et al., 2017):

$$157 \quad T_g = A + BM + C^2M^2 + D (\text{O:C}) + E M (\text{O:C}) \quad (1)$$

158 where  $A = -21.57 (\pm 13.47)$  [K],  $B = 1.51 (\pm 0.14)$  [K mol  $\text{g}^{-1}$ ],  $C = -1.7 \times 10^{-3} (\pm 3.0 \times 10^{-4})$  [K  
159  $\text{mol}^2 \text{g}^{-2}$ ],  $D = 131.4 (\pm 16.01)$  [K] and  $E = -0.25 (\pm 0.085)$  [K mol  $\text{g}^{-1}$ ], respectively. These values  
160 were obtained by fitting the measured  $T_g$  of 179 CH and CHO compounds with  $M < 450$  g  $\text{mol}^{-1}$   
161 with multi-linear least squares analysis. Note that application of Eq. (1) may provide  
162 unreasonable  $T_g$  values for compounds with  $M > 500$  g  $\text{mol}^{-1}$  because it does not account for the  
163 strong curvature in the  $T_g$  vs.  $M$  dependence shown in Figure 1a.

164 In this study we have developed an improved parameterization to predict  $T_g$  of CH and  
165 CHO compounds using the number of carbon ( $n_C$ ), hydrogen ( $n_H$ ), and oxygen ( $n_O$ ) that can also  
166 be applied to higher molar mass compounds. Motivated by a good correlation between  $T_g$  and  
167 volatility (Fig. 1a in Shiraiwa et al., (2017)), we use an equation with a similar formulation to the  
168 equation used to predict the saturation mass concentration or volatility (Donahue et al., 2011; Li  
169 et al., 2016):

$$170 \quad T_g = (n_C^0 + \ln(n_C)) b_C + \ln(n_H) b_H + \ln(n_C) \ln(n_H) b_{CH} + \ln(n_O) b_O + \ln(n_C) \ln(n_O) b_{CO} \quad (2)$$

171 where  $n_C^0$  is the reference carbon number,  $b_C$ ,  $b_H$  and  $b_O$  denote the contribution of each atom to  
172  $T_g$ , and  $b_{CH}$  and  $b_{CO}$  are coefficients that reflect contributions from carbon-hydrogen and carbon-  
173 oxygen bonds, respectively. These values were obtained by fitting the measured  $T_g$  of 42 CH  
174 compounds and 258 CHO compounds with multi-linear least squares analysis with 68%  
175 prediction and confidence intervals. The best-fit parameters are summarized in Table 1.

176 Note that the evaluation dataset used to derive Eq. (2) contains CH compounds with  $M <$   
177  $260 \text{ g mol}^{-1}$  (see Fig. A2b for comparison of measured and predicted  $T_g$ ). Thus, the application of  
178 Eq. (2) to higher molar mass compounds may require further investigations when measured  $T_g$   
179 for higher molar mass compounds becomes available. [We plan to continue to refine our method](#)  
180 [as additional glass transition data on high molar mass compounds become available.](#) Figure 1c  
181 shows that the  $T_g$  values predicted using Eq. (2) are in good agreement with the  $T_g$  values  
182 measured in experiments (see also Fig. A1(b)) or estimated by the Boyer-Kauzmann rule as  
183 indicated by the high correlation coefficient of 0.95.  $T_g$  of individual compounds can be  
184 predicted within  $\pm 21 \text{ K}$  as indicated by the prediction band (dotted lines in Fig. 1c); however,  
185 this uncertainty may be much smaller for multicomponent SOA mixtures under ideal mixing  
186 conditions as indicated in the confidence band (dashed lines, almost overlapping with the 1:1  
187 line).

188 These results are noteworthy given that the parameterization (Eq. 2) does not consider  
189 either explicit molecular structures or functional groups. Previous studies have shown that  $T_g$  can  
190 be especially sensitive to the number of OH groups, which interact strongly through hydrogen  
191 bonding. For example, Nakanishi et al., (2011) found a direct relationship between  $T_g$  and the  
192 number of hydroxyl groups in a molecule for sugar alcohols;  $T_g$  increases as the number of OH  
193 groups increases. They reported that the correlation between  $T_g$  and the number of OH groups  
194 was much stronger than the correlation between  $T_g$  and the number of carbons in a molecule.  
195 Such a trend is implicitly included in Eq. (1) and (2), which contain the O:C ratio and number of  
196 oxygen atoms as parameters, respectively. Recently, Rothfuss and Petters (2017) showed an  
197 approximately linear relationship between the number of OH groups and  $T_g$  for compounds with  
198 up to eight OH groups. Grayson et al. (2017) showed that addition of hydroxyl functional groups

199 increases viscosity, a conclusion supported by both the experimental data and quantitative  
200 structure-property relationship model. The correlation between  $T_g$  and the number of carbon  
201 atoms is consistent with the free volume theory, in which molecular motion is restricted by the  
202 difference between the space required for a molecule to vibrate versus the space in which the  
203 molecule resides (i.e., the free volume) (White and Lipson, 2016). The correlation between  $T_g$   
204 and the number of OH groups is more consistent with the topological constraint theory, where  
205 the primary influence is the three dimensional structure of the molecule as determined by  
206 molecular bonds and hydrogen-bonding networks (Nakanishi and Nozaki, 2011; van der Sman,  
207 2013). Future experiments targeting more comprehensive  $T_g$  data, especially for higher molar  
208 mass compounds, would lead to further refinements of our  $T_g$  parameterizations.

209 Comparing Eq. (1) and (2), the two parameterizations give similar performance for  
210 compounds with  $M < 450 \text{ g mol}^{-1}$  as shown in Fig. A2c. The statistical measures of correlation  
211 coefficient (R), mean bias (MB), and root mean square error (RMSE) are 0.93,  $-6.45 \text{ K}$ , and  
212  $25.64 \text{ K}$ , respectively, for the performance of Eq. (1), while for Eq. (2), they are 0.95,  $3.15 \text{ K}$ ,  
213 and  $21.11 \text{ K}$ , respectively. It should be noted again that Eq. (1) cannot be used to predict  $T_g$  for  
214 compounds with  $M > 450 \text{ g mol}^{-1}$ . For example,  $T_g$  of stachyose ( $M = 667 \text{ g mol}^{-1}$ ) predicted by  
215 Eq. (1) is  $198 \text{ K}$ , while that by Eq. (2) is  $394 \text{ K}$ , which agrees much better with the measured  
216 mean  $T_g$  of  $396 \text{ K}$  (Rothfuss and Petters, 2017). Eq. (2) is more flexible than Eq. (1) and can be  
217 potentially expanded to include compounds containing hetero-atoms (e.g., nitrogen or sulfur),  
218 once substantial sets of experimental values of  $T_g$  for such compounds become available.  
219 Regarding the application in air quality and climate models, Eq. (1) can be applied in the  
220 volatility basis set (VBS) (Donahue et al., 2006; Donahue et al., 2011) and the molecular  
221 corridor approach (Shiraiwa et al., 2014; Li et al., 2016) to predict the  $T_g$  of SOA particles

222 (Shiraiwa et al., 2017), while the new parameterization may be suitable for coupling with the  
 223 statistical oxidation model which characterizes the SOA evolution as a function of  $n_C$  and  $n_O$   
 224 (Cappa and Wilson, 2012; Jathar et al., 2015).

225 These parameterizations (Eqs. 1, 2) calculate  $T_g$  based on the elemental composition of  
 226 organic compounds. SOA particles contain a number of organic compounds as well as a variable  
 227 amount of liquid water, which has low  $T_g$  (136 K) and can act as a plasticizer (Mikhailov et al.,  
 228 2009; Koop et al., 2011). Under humid conditions, SOA particles take up water by hygroscopic  
 229 growth in response to RH, lowering  $T_g$  and viscosity of SOA particles. Estimations of  $T_g$  for  
 230 SOA-water mixtures were discussed by Shiraiwa et al. (2017), who applied the Gordon-Taylor  
 231 equation validated for a wide range of mixtures of organics, polymer, and water (Roos, 1993;  
 232 Hancock and Zografis, 1994; Zobrist et al., 2008; Dette et al., 2014; Dette and Koop, 2015).  
 233 Briefly,  $T_g$  of mixtures of SOA compounds under dry conditions ( $T_{g,org}$ ) were calculated  
 234 assuming the Gordon-Taylor constant ( $k_{GT}$ ) of 1 (Dette et al., 2014):  $T_{g,org} = \sum_i w_i T_{g,i}$ , where  $w_i$  is  
 235 the mass fraction of organic compound  $i$ , which can be derived using mass concentrations of  
 236 SOA products. The Gordon-Taylor equation can also be applied to calculate  $T_g$  of organic-water  
 237 mixtures considering the mass fraction of organics ( $w_{org}$ ) in SOA particles (Koop et al., 2011):

$$238 \quad T_g(w_{org}) = \frac{(1-w_{org})T_{g,w} + \frac{1}{k_{GT}}w_{org}T_{g,org}}{(1-w_{org}) + \frac{1}{k_{GT}}w_{org}} \quad (3)$$

239  $w_{org}$  can be calculated using the mass concentrations of water ( $m_{H_2O}$ ) and SOA ( $m_{SOA}$ ) as  $w_{org} =$   
 240  $m_{SOA} / (m_{SOA} + m_{H_2O})$ .  $m_{H_2O}$  can be estimated using the effective hygroscopicity parameter ( $\kappa$ )  
 241 (Petters and Kreidenweis, 2007):

$$242 \quad m_{H_2O} = \frac{\kappa \rho_w m_{SOA}}{\rho_{SOA} \left( \frac{1}{a_w} - 1 \right)} \quad (4)$$

243 The density of water ( $\rho_w$ ) is  $1 \text{ g cm}^{-3}$ , the density of SOA particles ( $\rho_{\text{SOA}}$ ) is assumed to be  $1.2 \text{ g}$   
244  $\text{cm}^{-3}$  (Kuwata et al., 2012),  $m_{\text{SOA}}$  is the total mass concentrations of SOA, and  $a_w$  is the water  
245 activity calculated as  $a_w = \text{RH}/100$ . Pajunoja et al. (2015) found that water uptake in subsaturated  
246 conditions is inhibited until RH is high enough for dissolution of water in SOA particles with  
247 relatively low O:C ratios. As oxidation of SOA increases, solubility of water increases and  
248 dissolution occurs at lower RH values. In both cases, the use of subsaturated hygroscopicity  
249 measurements was supported.

250

## 251 **2.2 Viscosity**

252 Temperature dependence of viscosity ( $\eta$ ) was predicted using the modified Vogel-  
253 Tamman-Fulcher (VTF) equation (Angell, 1991):

$$254 \quad \eta = \eta_{\infty} e^{\frac{T_0 D}{T - T_0}} \quad (5)$$

255 where  $\eta_{\infty}$  is viscosity at infinite temperature;  $T_0$  is the Vogel temperature;  $T$  is the ambient  
256 temperature. The fragility parameter,  $D$ , characterizes how rapidly the dynamics of a material  
257 slow down as  $T$  approaches  $T_g$ , reflecting to what degree the temperature dependence of the  
258 viscosity deviates from Arrhenius behavior. When  $T$  is close to  $T_g$  ( $T_g/T \approx 1$ ), smaller  $D$  values  
259 indicate that viscosity is sensitive to temperature change (fragile behavior); while larger  $D$  values  
260 indicate that viscosity is less sensitive to temperature change (strong or Arrhenius behavior).

261 Assuming  $\eta_{\infty} = 10^{-5} \text{ Pa s}$  (Angell, 1991):

$$262 \quad \log \eta = -5 + 0.434 \frac{T_0 D}{T - T_0} \quad (6)$$

263 When  $T = T_g$ ,  $\eta = 10^{12} \text{ Pa s}$ , which leads to (Angell, 1991; Angell, 2002):

$$264 \quad T_0 = \frac{39.17 T_g}{D + 39.17} \quad (7)$$

265 As can be seen in Eq. (5), both  $T_g$  and  $D$  are required to calculate  $\eta$  from Eq. (4) at a given  
266 temperature.

267 Figure 2 shows the  $T_g$ -scaled Arrhenius plot of fragility (viscosity versus  $T_g/T$ ) referred to  
268 as an Angell plot (Angell, 1995).  $D$  values of organic compounds are typically in the range of  
269 ~5–30 (Angell, 1997). To estimate  $D$  values that could be applied to SOA compounds, we  
270 compiled measured fragility values. Fragility was often measured in the form of the fragility  
271 steepness index ( $m$ ), which represents the slope of the Arrhenius plot at the point where  $T = T_g$   
272 (Boehmer et al., 1993). Compounds with lower  $m$  exhibit higher  $D$  values, indicating stronger  
273 glass formers. The measured  $m$  of 95 organic compounds are included in the Supplement.  $m$  can  
274 be converted to  $D$  using the following equation (see the full derivation of this equation in  
275 Appendix A):

$$276 \quad D = \frac{665.89}{m-17} \quad (8)$$

277 Figure 3 shows the measured  $D$  as a function of (a) molar mass and (b) atomic O:C ratio  
278 of organic molecules. The molar mass exerts a stronger effect on fragility, while there is little  
279 dependence of  $D$  on the O:C ratio. As molar mass increases,  $D$  approaches a lower limit of 10.3  
280 ( $\pm 1.7$ ), consistent with the value of 10 used in our recent study (Shiraiwa et al., 2017). To  
281 evaluate the impact of the variations of  $D$  on viscosity prediction, sensitivity calculations were  
282 conducted as described in Sect. 3.

283 Besides the VTF equation, another commonly used equation for describing the  
284 temperature dependence of viscosity is the Williams-Landel-Ferry (WLF) equation:  $\log \frac{\eta(T)}{\eta(T_g)} =$   
285  $\frac{-C_1(T-T_g)}{C_2+(T-T_g)}$ , where empirical parameters  $C_1$  and  $C_2$  are adopted as 17.44 and 51.6 K, respectively  
286 (Williams et al., 1955; Schill and Tolbert, 2013; Wang et al., 2015). The two equations are



287 mathematically equivalent, both defined with respect to a reference temperature, and their  
288 parameters are related through  $C_1 = \frac{DT_0}{2.303(T_g - T_0)}$  and  $C_2 = T_g - T_0$ . For the WLF equation,  $T_g$  is  
289 the reference temperature and there is a linear dependence assumed between temperature and  
290 free volume (O'Connell and McKenna, 1999; Huang and McKenna, 2001; Metatla and Soldera,  
291 2007). For the VTF equation, the reference is the Vogel temperature ( $T_0$ )—a hypothetical  
292 temperature at which all non-vibrational motion ceases and viscosity becomes infinite and the  
293 theoretical foundation of the VTF equation includes both thermodynamic and kinetic  
294 considerations (O'Connell and McKenna, 1999; Huang and McKenna, 2001; Metatla and  
295 Soldera, 2007). The calculations of viscosity in this study are based mainly on the VTF equation  
296 and the difference between calculated results from the two equations will be briefly discussed in  
297 the following section.

298

### 299 **3. Comparison of predicted viscosity with measurements**

#### 300 **3.1. SOA formed from $\alpha$ -pinene and isoprene**

301 The purpose of this section is to demonstrate that viscosity of SOA material can be  
302 predicted over a broad range of RH values from four parameters:  $T_g$  of dry SOA ( $T_{g,org}$ ), fragility  
303 ( $D$ ), hygroscopicity ( $\kappa$ ), and the Gordon-Taylor constant for mixing SOA and water ( $k_{GT}$ ).  
304 Viscosity of  $\alpha$ -pinene SOA has been measured as a function of RH by several groups using  
305 multiple experimental techniques as shown in Fig. 4(a) (Abramson et al., 2013; Renbaum-Wolff  
306 et al., 2013; Kidd et al., 2014; Pajunoja et al., 2014; Bateman et al., 2015; Zhang et al., 2015;  
307 Grayson et al., 2016). The wide range of experimentally measured viscosities reported for  $\alpha$ -  
308 pinene SOA, particularly from 30-60% RH is most likely a consequence of the different  
309 experimental approaches, mass loadings and O:C ratios for each experiment. For instance,

310 Grayson et al. (2016) used mass loadings of 121 to 14000  $\mu\text{g m}^3$  and observed that viscosity  
311 decreased as mass loading increased. Higher mass loadings would lead to greater partitioning of  
312 semi-volatile and lower molar mass compounds into the particle phase, which would lead to the  
313 decrease of  $T_g$  and viscosity of the resulting SOA mixture. They concluded that their results  
314 should be considered a lower limit for viscosity of  $\alpha$ -pinene SOA in the atmosphere. It should  
315 also be noted that the viscosity measurements from Renbaum-Wolff et al. (2013) were for the  
316 water-soluble portion of the SOA. These datasets suggest that viscosity of  $\alpha$ -pinene SOA  
317 approaches very high values ( $\sim 10^8$  Pa s) below 20-30% RH and decreases with an increase in  
318 RH reaching a value of  $\sim 10$  Pa s at 80% RH. As can be seen in Fig. 4(b), isoprene SOA is less  
319 viscous with  $\eta < 10^6$  Pa s even under dry conditions, undergoing a phase transition from a semi-  
320 solid phase to a liquid phase at  $\sim 55\%$  RH (Bateman et al., 2015; Song et al., 2015).

321 The solid lines with the shaded areas in Figure 4 are viscosity values predicted using  
322  $T_{g,\text{org}}$ ,  $D$ ,  $\kappa$ ,  $k_{GT}$ .  $T_{g,\text{org}}$  values were adopted by Berkemeier et al. (2014) who estimated  $T_{g,\text{org}}$  with  
323 the Boyer-Kauzmann rule using the melting point of representative SOA oxidation products.  
324 Note that Eq. (1) or (2) were not used to estimate  $T_{g,\text{org}}$ , which should be done in future studies  
325 by obtaining their elemental composition using high resolution mass spectrometry. For  $\alpha$ -pinene,  
326  $T_{g,\text{org}}$  was assumed to be 278 K corresponding to an O:C ratio of 0.5 (Berkemeier et al., 2014),  
327 which is a typical O:C ratio of  $\alpha$ -pinene SOA (Aiken et al., 2008; Chen et al., 2011; Putman et  
328 al., 2012).

329 The  $T_{g,\text{org}}$  selected for isoprene SOA was 255 K, corresponding to the O:C ratio of 0.6.  
330 Although no measurements of the O:C ratio for the experimental isoprene SOA data were  
331 reported, Song et al. (2015) estimated O:C of 0.64-1.1 based on literature values. As O:C ratios  
332 are useful in estimating  $T_{g,\text{org}}$ , we encourage the measurement of the O:C ratio of SOA when

333 conducting viscosity measurements. In contrast to  $\alpha$ -pinene SOA, there are limited viscosity  
334 measurements for isoprene SOA. While the predicted viscosity is consistent with the  
335 experimental data, comparison of our model predictions to additional measurements is strongly  
336 recommended. Song et al. (2015) prepared their samples in a potential aerosol mass (PAM)  
337 reactor while those investigated by Bateman et al. (2015) were generated in a smog chamber. It  
338 has been suggested that under ambient conditions, the majority of isoprene-derived SOA can be  
339 derived through heterogeneous interactions with acidic sulfate particles forming oligomers (Lin  
340 et al., 2013; Surratt et al., 2010; Gaston et al., 2014), which may increase viscosity. Further  
341 studies are warranted to compare laboratory-generated and ambient isoprene SOA, and to  
342 investigate the effect of the acidic seed on the viscosity.

343 For both  $\alpha$ -pinene and isoprene SOA,  $D$  was set to 10 based on the analysis presented in  
344 Fig. 3(a).  $\kappa$  was set to 0.1 based on field and laboratory measurements (Gunthe et al., 2009;  
345 Lambe et al., 2011b; Pajunoja et al., 2014; Petters et al., 2017) and  $k_{GT}$  was assumed to be 2.5  
346 (Zobrist et al., 2008; Koop et al., 2011). Using these parameters, the predicted viscosities match  
347 well the magnitude and the RH-dependence of the measured viscosity of  $\alpha$ -pinene and isoprene  
348 SOA. Figure 4 also shows predicted viscosities (dotted lines) using the WLF equation, which  
349 shows similar values as the VTF equation, but slightly underestimates the viscosity of  $\alpha$ -pinene  
350 SOA at low RH and overestimates the viscosity of isoprene SOA at high RH.

351 Sensitivity studies were conducted to examine the effects of  $T_{g,org}$ ,  $D$ ,  $\kappa$  and  $k_{GT}$ , on the  
352 calculated viscosity. In these studies,  $T_{g,org}$  of  $\alpha$ -pinene and isoprene SOA were varied within  
353 229-328 K and 255-316 K, respectively, representing  $T_{g,org}$  of different oxidation states  
354 (Berkemeier et al., 2014).  $D$  was varied between 5 and 30, which is the range characteristic for  
355 organic compounds (see Fig. 3a).  $\kappa$  of 0.05-0.15 were used for  $\alpha$ -pinene and isoprene SOA

356 (Lambe et al., 2011b; Pajunoja et al., 2015). For the Gordon-Taylor constant, values of  $2.5 \pm 1.5$   
357 were considered (Zobrist et al., 2008; Koop et al., 2011; Dette et al., 2014; Dette and Koop,  
358 2015).

359 The effect of varying each parameter on the calculated viscosity of  $\alpha$ -pinene SOA is  
360 illustrated in Fig. 5. Variations of  $\pm 50$  K in  $T_{g,org}$  result in 3-6 orders of magnitude difference in  
361 calculated values at dry conditions, indicating that  $T_{g,org}$  is a critical parameter for viscosity  
362 estimations. Decreasing  $D$  from 10 to 5 led to a decrease of calculated values by more than one  
363 order of magnitude. The calculated results were within the upper limit of measurements when  
364 increasing  $D$  from 10 to 20, and the predicted values were only slightly enhanced when further  
365 increasing  $D$  from 20 to 30. Calculated values with variations in  $\kappa$  from 0.05 to 0.15 and  $k_{GT}$   
366 from 1.0 to 4.0 were all within the measured ranges.

367 For isoprene SOA, an increase of  $T_{g,org}$  to 287 K, which represents a higher oxidation  
368 state (Berkemeier et al., 2014), led to calculated values to be several orders of magnitude higher  
369 than the upper limit of measurements (Fig. 6a). When  $T_{g,org}$  reaches 316 K, isoprene SOA can  
370 occur as a solid for RH lower than  $\sim 40\%$ . Compared to  $\alpha$ -pinene SOA, a variation in  $D$  has a  
371 larger effect on the calculated viscosity (Fig. 6b). For a range of 5 - 30 for  $D$ , calculations with  
372 the  $D$  value of 10 agreed well with the measurements, while other  $D$  values resulted in calculated  
373 viscosity outside of the measured ranges. Figures 6c and 6d show that decreasing  $\kappa$  and  $k_{GT}$   
374 below the reference values, the predictions overestimate the measured  $\eta$  by one or two orders of  
375 magnitude. The latter is most evident at RH  $> 60\%$ , where the calculated values were higher than  
376 the upper limit of measurements. Modeling results with  $\kappa$  and  $k_{GT}$  increasing to 0.15 and 4.0,  
377 respectively, were within the lower limit of measurements.

378           The above comparison between the measured and predicted viscosity demonstrates that  
379 the method described in this study can reproduce reasonably well the measured RH-dependent  
380 viscosity of SOA formed from  $\alpha$ -pinene and isoprene. The sensitivity calculations showed that  
381  $T_{g,org}$  contributed the most to the uncertainty in the viscosity estimates. Previous studies have  
382 shown that the experimental conditions such as particle mass concentrations (Grayson et al.,  
383 2016) and RH upon SOA formation (Kidd et al., 2014; Hinks et al., 2018) can impact chemical  
384 composition of SOA and hence the [phase state and](#) viscosity. Further efforts to constrain the  
385 uncertainties are needed both in experiments and parameterizations.

386

### 387 **3.2. SOA formed from toluene**

388           In this and the following sections, we examine the feasibility of calculating the value of  
389  $T_{g,org}$  from mass spectrometry data on SOA. Hinks et al. (2017) measured the elemental  
390 composition of toluene SOA using nanospray desorption electrospray ionization high-resolution  
391 mass spectrometry (nano-DESI-HRMS) (Roach et al., 2010a, b). Toluene SOA were formed by  
392 OH photooxidation in an aerosol smog chamber at <2% RH (mass loading =  $23 \mu\text{g m}^{-3}$ ) and 75%  
393 RH (mass loading =  $8 \mu\text{g m}^{-3}$ ) to investigate the effect of RH on the chemical composition of  
394 toluene SOA formed under low- $\text{NO}_x$  conditions. Measurements revealed a significant reduction  
395 in the fraction of oligomers present in toluene SOA generated under high RH conditions  
396 compared to SOA generated under low RH conditions (Hinks et al., 2017). The detected molar  
397 mass of individual oxidation products spanned a range of  $102 - 570 \text{ g mol}^{-1}$  at high RH, which  
398 increased up to  $726 \text{ g mol}^{-1}$  at low RH.

399           Figure 7(a) shows the interdependence of glass transition temperature, volatility, and  
400 molar mass of the detected toluene SOA compounds. Glass transition temperatures were

401 calculated using Eq. (2). Saturation mass concentrations or volatilities of detected compounds  
402 were estimated from the elemental composition by using the parameterization of Li et al. (2016).  
403 The analysis is based on the molecular corridor approach—a two-dimensional framework of  
404 volatility and molar mass of SOA components constrained by boundary lines of low and high  
405 atomic O:C ratio, corresponding to *n*-alkanes ( $C_nH_{2n+2}$ , O:C = 0) and sugar alcohols ( $C_nH_{2n+2}O_n$ ,  
406 O:C = 1), respectively (Shiraiwa et al., 2014; Li et al., 2016). The toluene SOA constituents are  
407 well constrained by the molecular corridor and  $T_g$  are higher for compounds with higher molar  
408 mass and lower volatility.

409 Eq. (1) was used to calculate  $T_g$  for individual compounds with  $M < 450 \text{ g mol}^{-1}$ , while  
410 excluding compounds with molar mass higher than  $450 \text{ g mol}^{-1}$ . This approach was deemed  
411 reasonable as such high molar mass compounds account for < 10% of all toluene SOA products  
412 formed at low RH, and for < 2% formed at high RH. Eq. (2) was used to calculate  $T_g$  for all the  
413 detected compounds.  $T_g$  of dry toluene SOA ( $T_{g,org}$ ) was then computed using the Gordon-Taylor  
414 approach with  $k_{GT} = 1$  (Sect. 2.1). The relative mass concentrations of individual components  
415 were assumed to be proportional to their relative abundance in the nano-DESI-HRMS spectrum.  
416 This assumption has a number of caveats (Bateman et al., 2012; Nguyen et al., 2013), and as we  
417 will see below, it results in deviations between the predicted and measured viscosity. Table 2  
418 summarizes the results of such calculations, showing that the  $T_{g,org}$  by Eq. (1) – excluding high  
419 molar mass compounds – is about 10 K lower as compared to  $T_{g,org}$  by Eq. (2).  $T_{g,org}$  at low RH is  
420 predicted to be higher than  $T_{g,org}$  at high RH, which results from a lower abundance of high molar  
421 mass compounds observed at high RH. This trend is consistent with Kidd et al. (2014), who  
422 showed that SOA material formed under dry conditions is more viscous than that formed under  
423 wet conditions.

424 Figure 7(b) shows the predicted viscosity of toluene SOA as a function of RH, as  
425 compared to the measured viscosity of toluene SOA formed in an oxidation flow reactor at 13%  
426 RH (Song et al., 2016a). Indirect viscosity measurements are also included in shaded boxes  
427 (Bateman et al., 2015; Li et al., 2015). Lines with shaded areas are calculated viscosities using  
428  $T_{g,org}$  as described above.  $\kappa$  was assumed to be 0.25 based on laboratory measurements (Lambe et  
429 al., 2011a; Hildebrandt Ruiz et al., 2015). To achieve good fit,  $D$  was set to 13 and  $k_{GT}$  was  
430 assumed to be 3.0 (Dette et al., 2014). Estimations with Eq. (1) match the measured viscosity  
431 values very well over the entire RH range. Predictions with Eq. (2) overestimated the  
432 measurements by one or two orders of magnitude at moderate RH between 30% and 50%, while  
433 they agreed with the measurements derived at  $RH \geq 60\%$  and at the dry conditions.

434 There are several possible reasons for the difference between the measurements and  
435 predictions. First, the relative abundance of high molar mass compounds observed in HRMS  
436 measurements may be overestimated, as high molar mass compounds tend to have higher (yet  
437 generally unknown) ionization efficiencies compared to lower molar mass compounds. Second,  
438 the nano-DESI-HRMS analysis of toluene SOA was limited to  $m/z$  range of 100 -1000 (Hinks et  
439 al., 2017). It is possible that some SOA products with lower molar mass were present in particles  
440 but not detected, which would lead to an overestimation of  $T_g$ . Third, the chemical composition  
441 of toluene SOA are likely different between Hinks et al. (2017) and Song et al. (2016) because of  
442 the differences in the experimental conditions. Specifically, toluene SOA was formed in a Teflon  
443 chamber in Hinks et al., while Song et al. used an oxidation flow reactor to generate toluene  
444 SOA. The O:C ratios are 0.71 at low RH and 0.63 at high RH based on nano-DESI-HRMS  
445 measurements in Hinks et al. (2017), while it was 1.06 based on the aerosol mass spectrometry  
446 (AMS) measurements in Song et al. (2016).

447 In addition, different mass loadings may have affected viscosity. Song et al. (2016)  
448 measured viscosity at two different mass loadings (60-100 and 600-1000  $\mu\text{g m}^{-3}$ ) and compared  
449 their results to Bateman et al. (2015) (30-50  $\mu\text{g m}^{-3}$ ) and Li et al. (2015) (44-125  $\mu\text{g m}^{-3}$ ),  
450 observing little impact of mass loadings on viscosity. We carried out a sensitivity study of mass  
451 loadings on viscosity using a set of compounds detected by HRMS. The saturation mass  
452 concentration was predicted for each component using the molecular corridor approach (Li et al.,  
453 2016). Assuming that the mass signal intensity is proportional to the total mass concentration of  
454 the compound in the mixture, and applying the absorptive partitioning theory (Pankow, 1994),  
455 particle-phase concentrations of each compound were predicted to estimate  $T_g$  at different  
456 organic aerosol mass loading values (1-1000  $\mu\text{g m}^{-3}$ ). The glass transition temperature of the  
457 SOA mixture decreases as mass loading increases. Viscosity decreases up to two orders of  
458 magnitude at low RH, while at high RH they have little difference as shown in Fig. A3.  
459 Simultaneous measurements of viscosity and chemical composition with different mass loadings  
460 should be performed in future studies.

461

### 462 **3.3 Biomass Burning Particles**

463 To further explore the applicability of our viscosity prediction method using elemental  
464 composition as measured by HRMS, we performed similar calculations for biomass burning  
465 organic particles emitted from test facility burns of subalpine fir and lodgepole pine trees,  
466 conducted as a part of the FIREX 2016 campaign (Selimovic et al., 2017). These samples were  
467 analyzed by HRMS using two different ionization sources: electrospray ionization (ESI) and  
468 atmospheric pressure photoionization (APPI). Mass spectra shown in Fig. 8(a) and (b) indicate  
469 that a substantial number of compounds were detected by both methods (109 and 170



470 compounds for subalpine fir and lodgepole pine, respectively). However, pronounced  
471 differences are also observed between the ESI and APPI spectra both in terms of the identity and  
472 signal intensities of the detected compounds.

473 Glass transition temperatures for the assigned CH and CHO compounds were computed  
474 using Eq. (2). Nitrogen and sulfur containing compounds (CHON and CHOS) are not yet  
475 covered by Eq. (2) and were therefore excluded from the analysis. CHON and CHOS compounds  
476 comprised less than 10% of the detected ion intensity and <15% of the assigned compounds.  
477 Please note that we do not intend to provide accurate estimates of ambient biomass burning  
478 particles (as inorganic components are also not included in this analysis), but we investigate how  
479 the use of different ionization methods would lead to variations in our viscosity predictions.  $T_g$  of  
480 organic mixtures ( $T_{g,org}$ ) were then calculated using the Gordon-Taylor approach with  $k_{GT} = 1$ ,  
481 assuming that the relative concentration of each compound is proportional to its MS signal  
482 intensity. The calculated  $T_{g,org}$  values for the mixtures are specified in the legend of Figure 9. For  
483 both types of mixtures, the calculated  $T_{g,org}$  for the APPI MS data is lower than the value  
484 calculated based on the ESI MS data with a difference of 32 K for subalpine fir and 11 K for the  
485 lodgepole pine. Figure 9 shows the predicted viscosity as a function of RH, assuming  $D = 10$ ,  $\kappa$   
486 = 0.10 and  $k_{GT} = 2.5$ . The difference in  $T_{g,org}$  derived from ESI and APPI results in a variation of  
487 predicted viscosity at low RH by up to five and two orders of magnitude for subalpine fir and  
488 lodgepole pine, respectively.

489 The difference in the calculated  $T_{g,org}$  values is attributed to the chemical profile of the  
490 species detected using different ionization techniques as shown in mass spectra in Fig. 8(a) and  
491 (b). Van Krevelen diagrams in Fig. 8(c) and (d) illustrate these compositional differences  
492 between chemical species detected by ESI and APPI. ESI is more efficient at detection of polar

493 compounds (Kiontke et al., 2016), which typically have higher O:C ratios and therefore would  
494 result in higher predicted values of viscosity (Koop et al., 2011; Saukko et al., 2012). APPI  
495 enables the detection of nonpolar compounds with lower O:C ratios, in particular polycyclic  
496 aromatic hydrocarbons (PAHs), that have low ionization efficiencies when analyzed by ESI MS  
497 (Raffaelli and Saba, 2003; Itoh et al., 2006). Due to the complementary nature of these ionization  
498 methods, it is most likely that the actual glass transition temperature and viscosity of each type of  
499 SOA are somewhere in between the values inferred from ESI and APPI data sets: ESI MS may  
500 be viewed as providing the upper limit of viscosity, while APPI MS gives the lower limit. Our  
501 results indicate that the use of complementary ionization techniques may help evaluate the  
502 associated uncertainty for the prediction of viscosity values based on the elemental composition  
503 as measured by HRMS.

504

#### 505 **4 Conclusions**

506 We have developed a parameterization for calculation of the glass transition temperature  
507 of individual SOA compounds with molar mass up to  $\sim 1100 \text{ g mol}^{-1}$  using the number of carbon,  
508 oxygen, and hydrogen atoms. Viscosity of SOA was estimated using the  $T_g$ -scaled Arrhenius plot  
509 of viscosity versus  $T_g/T$  and the Gordon-Taylor approach to account for mixtures of SOA and  
510 water. The fragility parameter  $D$  was compiled for organic compounds and we found that  $D$   
511 approaches a lower limit of  $\sim 10$  ( $\pm 1.7$ ) as the molar mass increases. The resulting viscosity  
512 estimations agree well with measured viscosity of  $\alpha$ -pinene and isoprene SOA, validating our  
513 method. Using HRMS data, glass transition temperatures of individual components and viscosity  
514 of toluene SOA were predicted, also resulting in a good agreement with measurements.  
515 However, we note that the predicted viscosities were slightly higher than the measured values

516 suggesting that additional considerations may need to be taken into account. For example, the  
517 ionization efficiency of both low and high molar mass compounds may have a pronounced effect  
518 on the relative abundance of different classes of compounds in HRMS data. The viscosity  
519 prediction method was also applied to biomass burning particles, whose elemental composition  
520 was measured using HRMS with two different ionization techniques. Substantial differences in  
521 viscosity estimations were obtained using ESI and APPI mass spectra.

522 Figure 10 summarizes the predicted range of viscosity of  $\alpha$ -pinene SOA, isoprene SOA,  
523 toluene SOA, and biomass burning particles. Isoprene SOA has lower viscosity, reflecting lower  
524 glass transition temperature due to relatively low molar mass of isoprene oxidation products.  $\alpha$ -  
525 pinene and toluene SOA have much higher viscosity with a different shape of the RH  
526 dependence due to differences in glass transition temperatures and hygroscopicity. Biomass  
527 burning particles have moderate viscosity between the two extreme cases. Currently, both  
528 predictions and measurements are subject to large uncertainties and variations. Complementary  
529 measurements of viscosity and chemical composition employing different ionization techniques  
530 are desired to further constrain RH-dependent viscosity in future studies. Current  $T_g$   
531 parameterizations do not consider functionality or molecular structure explicitly and further  
532 measurements of  $T_g$  and viscosity of SOA would allow us to refine the method presented in this  
533 study. Nevertheless, current results offer a promising starting point and such simple  
534 parameterizations are practical for predicting viscosity of particles as measured by HRMS. The  
535 developed viscosity prediction method should also be useful in recent efforts of simulating the  
536 distribution of SOA phase state and related properties in regional or global air quality models  
537 (e.g., Maclean et al., 2017; Shiraiwa et al., 2017).

538

539 **Appendix A: Conversion of fragility steepness index ( $m$ ) to fragility ( $D$ )**

540 Fragility steepness index ( $m$ ) is defined as:

541 
$$m = \lim_{T \rightarrow T_g} \frac{d \log \eta}{d(T_g/T)} \quad (\text{A1})$$

542 Combining Eq. (A1) with Eq. (4) gives:

543 
$$m = \lim_{T \rightarrow T_g} \frac{d}{d(T_g/T)} \left( -5 + 0.434 \frac{T_0 D}{T - T_0} \right) \quad (\text{A2})$$

544 Considering that  $\eta = 10^{12}$  Pa s at  $T = T_g$  (Angell, 1991), and by defining  $\Delta x = 1 - T_g/T$ , and a  
545 combination with Eq. (5) leads to:

$$\begin{aligned} m &= \lim_{\Delta x \rightarrow 0} \frac{1}{\Delta x} \left( 12 - \left( -5 + 0.434 \frac{\frac{39.17 T_g D}{D + 39.17}}{\frac{T_g}{1 - \Delta x} - \frac{39.17 T_g}{D + 39.17}} \right) \right) \\ &= \lim_{\Delta x \rightarrow 0} \frac{1}{\Delta x} \left( 17 - 0.434 \frac{39.17 T_g D (1 - \Delta x)}{D T_g + 39.17 T_g \Delta x} \right) \\ &= \lim_{\Delta x \rightarrow 0} \frac{(665.89 + 17D)}{(D + 39.17 \Delta x)} \\ &= \frac{665.89 + 17D}{D} \quad (\text{A3}) \end{aligned}$$

547 Note that Eq. (A3) is derived assuming the high temperature limit of viscosity  $\eta_\infty$  is equal to  $10^{-5}$   
548 Pa s (Angell, 1991) in the VTF equation (Eq. 3). Similar equations for the relation between  $m$   
549 and  $D$  were given by previous studies using different  $\eta_\infty$  and units (Angell et al., 1994; Angell,  
550 2002; Bones et al., 2012) and applying those gave very similar results in our study.

551

552 **Acknowledgements.**

553 This work was funded by the National Science Foundation (AGS-1654104) and the Department  
554 of Energy (DE-SC0018349). The Purdue group and S. N. acknowledge additional support by the  
555 U.S. Department of Commerce, National Oceanic and Atmospheric Administration through

556 Climate Program Office's AC4 program, awards NA16OAR4310101 and NA16OAR4310102.

557 We thank Ulrich Pöschl and Thomas Koop for stimulating discussions.

558

559 **References.**

560 Abbatt, J. P. D., Lee, A. K. Y., and Thornton, J. A.: Quantifying trace gas uptake to tropospheric  
561 aerosol: recent advances and remaining challenges, *Chem. Soc. Rev.*, 41, 6555-6581, 2012.

562 Abramson, E., Imre, D., Beranek, J., Wilson, J., and Zelenyuk, A.: Experimental determination  
563 of chemical diffusion within secondary organic aerosol particles, *Physical Chemistry Chemical  
564 Physics*, 15, 2983-2991, 2013.

565 Aiken, A. C., DeCarlo, P. F., Kroll, J. H., et al.: O/C and OM/OC Ratios of Primary, Secondary,  
566 and Ambient Organic Aerosols with High-Resolution Time-of-Flight Aerosol Mass  
567 Spectrometry, *Environ. Sci. Technol.*, 42, 4478-4485, 2008.

568 Angell, C.: Relaxation in liquids, polymers and plastic crystals—strong/fragile patterns and  
569 problems, *Journal of Non-Crystalline Solids*, 131, 13-31, 1991.

570 Angell, C. A., Bressel, R. D., Green, J. L., Kanno, H., Oguni, M., and Sare, E. J.: Liquid fragility  
571 and the glass transition in water and aqueous solutions, *Journal of Food Engineering*, 22, 115-  
572 142, 1994.

573 Angell, C. A.: Formation of glasses from liquids and biopolymers, *Science*, 267, 1924-1935,  
574 1995.

575 Angell, C. A.: Entropy and fragility in supercooling liquids, National Institute of Standards and  
576 Technology, *Journal of Research*, 102, 171-185, 1997.

577 Angell, C. A.: Liquid Fragility and the Glass Transition in Water and Aqueous Solutions, *Chem.  
578 Rev.*, 102, 2627-2650, 2002.

579 Arangio, A. M., Slade, J. H., Berkemeier, T., Pöschl, U., Knopf, D. A., and Shiraiwa, M.:  
580 Multiphase Chemical Kinetics of OH Radical Uptake by Molecular Organic Markers of Biomass  
581 Burning Aerosols: Humidity and Temperature Dependence, *Surface Reaction and Bulk  
582 Diffusion*, *J. Phys. Chem. A*, 119, 4533-4544, 2015.

583 Bateman, A. P., Laskin, J., Laskin, A., and Nizkorodov, S. A.: Applications of High-Resolution  
584 Electrospray Ionization Mass Spectrometry to Measurements of Average Oxygen to Carbon  
585 Ratios in Secondary Organic Aerosols, *Environ. Sci. Technol.*, 46, 8315-8324, 2012.

586 Bateman, A. P., Bertram, A. K., and Martin, S. T.: Hygroscopic Influence on the Semisolid-to-  
587 Liquid Transition of Secondary Organic Materials, *J. Phys. Chem. A*, 119, 4386-4395, 2015.

- 588 Bateman, A. P., Gong, Z., Liu, P., et al.: Sub-micrometre particulate matter is primarily in liquid  
589 form over Amazon rainforest, *Nat. Geosci.*, 9, 34-37, 2016.
- 590 Baustian, K. J., Wise, M. E., Jensen, E. J., Schill, G. P., Freedman, M. A., and Tolbert, M. A.:  
591 State transformations and ice nucleation in amorphous (semi-)solid organic aerosol, *Atmos.*  
592 *Chem. Phys.*, 13, 5615-5628, 2013.
- 593 Berkemeier, T., Shiraiwa, M., Pöschl, U., and Koop, T.: Competition between water uptake and  
594 ice nucleation by glassy organic aerosol particles, *Atmos. Chem. Phys.*, 14, 12513-12531, 2014.
- 595 Berkemeier, T., Steimer, S., Krieger, U. K., Peter, T., Pöschl, U., Ammann, M., and Shiraiwa,  
596 M.: Ozone uptake on glassy, semi-solid and liquid organic matter and the role of reactive oxygen  
597 intermediates in atmospheric aerosol chemistry, *Phys. Chem. Chem. Phys.*, 18, 12662-12674,  
598 2016.
- 599 Boehmer, R., Ngai, K. L., Angell, C. A., and Plazek, D. J.: Nonexponential relaxations in strong  
600 and fragile glass formers, *J. Chem. Phys.*, 99, 4201-4209, 1993.
- 601 Bones, D. L., Reid, J. P., Lienhard, D. M., and Krieger, U. K.: Comparing the mechanism of  
602 water condensation and evaporation in glassy aerosol, *Proc. Natl. Acad. Sci. U.S.A.*, 109, 11613-  
603 11618, 2012.
- 604 Booth, A. M., Murphy, B., Riipinen, I., Percival, C. J., and Topping, D. O.: Connecting Bulk  
605 Viscosity Measurements to Kinetic Limitations on Attaining Equilibrium for a Model Aerosol  
606 Composition, *Environ. Sci. Technol.*, 48, 9298-9305, 2014.
- 607 Cappa, C. D., and Wilson, K. R.: Evolution of organic aerosol mass spectra upon heating:  
608 implications for OA phase and partitioning behavior, *Atmos. Chem. Phys.*, 11, 1895-1911, 2011.
- 609 Cappa, C. D., and Wilson, K. R.: Multi-generation gas-phase oxidation, equilibrium partitioning,  
610 and the formation and evolution of secondary organic aerosol, *Atmos. Chem. Phys.*, 12, 9505-  
611 9528, 2012.
- 612 Chen, Q., Liu, Y., Donahue, N. M., Shilling, J. E., and Martin, S. T.: Particle-Phase Chemistry of  
613 Secondary Organic Material: Modeled Compared to Measured O:C and H:C Elemental Ratios  
614 Provide Constraints, *Environ. Sci. Technol.*, 45, 4763-4770, 2011.
- 615 Davies, J. F., and Wilson, K. R.: Nanoscale interfacial gradients formed by the reactive uptake of  
616 OH radicals onto viscous aerosol surfaces, *Chem. Sci.*, 6, 7020-7027, 2015.
- 617 Dette, H. P., Qi, M., Schröder, D. C., Godt, A., and Koop, T.: Glass-forming properties of 3-  
618 Methylbutane-1,2,3-tricarboxylic acid and its mixtures with water and pinonic acid, *J. Phys.*  
619 *Chem. A*, 118, 7024-7033, 2014.
- 620 Dette, H. P., and Koop, T.: Glass Formation Processes in Mixed Inorganic/Organic Aerosol  
621 Particles, *J. Phys. Chem. A*, 119, 4552-4561, 2015.

622 Donahue, N. M., Robinson, A. L., Stanier, C. O., and Pandis, S. N.: Coupled partitioning,  
623 dilution, and chemical aging of semivolatile organics, *Environ. Sci. Technol.*, 40, 2635-2643,  
624 2006.

625 Donahue, N. M., Epstein, S. A., Pandis, S. N., and Robinson, A. L.: A two-dimensional volatility  
626 basis set: 1. organic-aerosol mixing thermodynamics, *Atmos. Chem. Phys.*, 11, 3303-3318, 2011.

627 Fox Jr, T. G., and Flory, P. J.: Second - order transition temperatures and related properties of  
628 polystyrene. I. Influence of molecular weight, *J. Appl. Phys.*, 21, 581-591, 1950.

629 Gao, S., Ng, N. L., Keywood, M., et al.: Particle phase acidity and oligomer formation in  
630 secondary organic aerosol, *Environ. Sci. Technol.*, 38, 6582-6589, 2004.

631 Goldstein, A. H., and Galbally, I. E.: Known and unexplored organic constituents in the earth's  
632 atmosphere, *Environ. Sci. Technol.*, 41, 1514-1521, 2007.

633 Gorkowski, K., Donahue, N. M., and Sullivan, R. C.: Emulsified and Liquid-Liquid Phase-  
634 Separated States of  $\alpha$ -Pinene Secondary Organic Aerosol Determined Using Aerosol Optical  
635 Tweezers, *Environ. Sci. Technol.*, 51, 12154-12163, 2017.

636 Grayson, J. W., Zhang, Y., Mutzel, A., Renbaum-Wolff, L., Böge, O., Kamal, S., Herrmann, H.,  
637 Martin, S. T., and Bertram, A. K.: Effect of varying experimental conditions on the viscosity of  
638  $\alpha$ -pinene derived secondary organic material, *Atmos. Chem. Phys.*, 16, 6027-6040, 2016.

639 Grayson, J. W., Evoy, E., Song, M., et al.: The effect of hydroxyl functional groups and molar  
640 mass on the viscosity of non-crystalline organic and organic-water particles, *Atmos. Chem.*  
641 *Phys.*, 17, 8509-8524, 2017.

642 Gunthe, S. S., King, S. M., Rose, D., et al.: Cloud condensation nuclei in pristine tropical  
643 rainforest air of Amazonia: size-resolved measurements and modeling of atmospheric aerosol  
644 composition and CCN activity, *Atmos. Chem. Phys.*, 9, 7551-7575, 2009.

645 Hancock, B. C., and Zograf, G.: The relationship between the glass transition temperature and  
646 the water content of amorphous pharmaceutical solids, *Pharm. Res.*, 11, 471-477, 1994.

647 Hildebrandt Ruiz, L., Paciga, A. L., Cerully, K. M., Nenes, A., Donahue, N. M., and Pandis, S.  
648 N.: Formation and aging of secondary organic aerosol from toluene: changes in chemical  
649 composition, volatility, and hygroscopicity, *Atmos. Chem. Phys.*, 15, 8301-8313, 2015.

650 Hinks, M. L., Brady, M. V., Lignell, H., et al.: Effect of viscosity on photodegradation rates in  
651 complex secondary organic aerosol materials, *Phys. Chem. Chem. Phys.*, 18, 8785-8793, 2016.

652 Hinks, M. L., Montoya-Aguilera, J., Ellison, L., Lin, P., Laskin, A., Laskin, J., Shiraiwa, M.,  
653 Dabdub, D., and Nizkorodov, S. A.: Effect of Relative Humidity on the Composition of  
654 Secondary Organic Aerosol from Oxidation of Toluene, *Atmos. Chem. Phys. Discuss.*, 2017, 1-  
655 16, 2017.

656 Hinks, M. L., Montoya-Aguilera, J., Ellison, L., Lin, P., Laskin, A., Laskin, J., Shiraiwa, M.,  
657 Dabdub, D., and Nizkorodov, S. A.: Effect of relative humidity on the composition of secondary  
658 organic aerosol from the oxidation of toluene, *Atmos. Chem. Phys.*, 18, 1643-1652, 2018.

659 Hosny, N. A., Fitzgerald, C., Vysniauskas, A., et al.: Direct imaging of changes in aerosol  
660 particle viscosity upon hydration and chemical aging, *Chem. Sci.*, 7, 1357-1367, 2016.

661 Huang, D., and McKenna, G. B.: New insights into the fragility dilemma in liquids, *J. Chem.*  
662 *Phys.*, 114, 5621-5630, 2001.

663 Huang, W., Saathoff, H., Pajunoja, A., Shen, X., Naumann, K. H., Wagner, R., Virtanen, A.,  
664 Leisner, T., and Mohr, C.:  $\alpha$ -Pinene secondary organic aerosol at low temperature: chemical  
665 composition and implications for particle viscosity, *Atmos. Chem. Phys.*, 18, 2883-2898, 2018.

666 Ignatius, K., Kristensen, T. B., Järvinen, E., et al.: Heterogeneous ice nucleation of viscous  
667 secondary organic aerosol produced from ozonolysis of  $\alpha$ -pinene, *Atmos. Chem. Phys.*, 16,  
668 6495-6509, 2016.

669 Itoh, N., Aoyagi, Y., and Yarita, T.: Optimization of the dopant for the trace determination of  
670 polycyclic aromatic hydrocarbons by liquid chromatography/dopant-assisted atmospheric-  
671 pressure photoionization/mass spectrometry, *J. Chromatogr. A*, 1131, 285-288, 2006.

672 Jain, S., and Petrucci, G. A.: A New Method to Measure Aerosol Particle Bounce Using a  
673 Cascade Electrical Low Pressure Impactor, *Aerosol Sci. Technol.*, 49, 390-399, 2015.

674 Jathar, S. H., Cappa, C. D., Wexler, A. S., Seinfeld, J. H., and Kleeman, M. J.: Multi-  
675 generational oxidation model to simulate secondary organic aerosol in a 3-D air quality model,  
676 *Geosci. Model Dev.*, 8, 2553-2567, 2015.

677 Jimenez, J. L., Canagaratna, M. R., Donahue, N. M., et al.: Evolution of organic aerosols in the  
678 atmosphere, *Science*, 326, 1525-1529, 2009.

679 Kidd, C., Perraud, V., Wingen, L. M., and Finlayson-Pitts, B. J.: Integrating phase and  
680 composition of secondary organic aerosol from the ozonolysis of alpha-pinene, *Proc. Natl. Acad.*  
681 *Sci. U.S.A.*, 111, 7552-7557, 2014.

682 Kiontke, A., Oliveira-Birkmeier, A., Opitz, A., and Birkemeyer, C.: Electrospray ionization  
683 efficiency is dependent on different molecular descriptors with respect to solvent ph and  
684 instrumental configuration, *PLoS One*, 11, e0167502/0167501-e0167502/0167516, 2016.

685 Knopf, D. A., Alpert, P. A., and Wang, B.: The Role of Organic Aerosol in Atmospheric Ice  
686 Nucleation: A Review, *ACS Earth and Space Chemistry*, 2018.

687 Koop, T., Bookhold, J., Shiraiwa, M., and Pöschl, U.: Glass transition and phase state of organic  
688 compounds: dependency on molecular properties and implications for secondary organic  
689 aerosols in the atmosphere, *Phys. Chem. Chem. Phys.*, 13, 19238-19255, 2011.



690 Kuwata, M., and Martin, S. T.: Phase of atmospheric secondary organic material affects its  
691 reactivity, *Proc. Natl. Acad. Sci. U.S.A.*, 109, 17354-17359, 2012.

692 Kuwata, M., Zorn, S. R., and Martin, S. T.: Using elemental ratios to predict the density of  
693 organic material composed of carbon, hydrogen, and oxygen, *Environ. Sci. Technol.*, 46, 787-  
694 794, 2012.

695 Lambe, A. T., Ahern, A. T., Williams, L. R., et al.: Characterization of aerosol photooxidation  
696 flow reactors: heterogeneous oxidation, secondary organic aerosol formation and cloud  
697 condensation nuclei activity measurements, *Atmos. Meas. Tech.*, 4, 445-461, 2011a.

698 Lambe, A. T., Onasch, T. B., Massoli, P., et al.: Laboratory studies of the chemical composition  
699 and cloud condensation nuclei (CCN) activity of secondary organic aerosol (SOA) and oxidized  
700 primary organic aerosol (OPOA), *Atmos. Chem. Phys.*, 11, 8913-8928, 2011b.

701 Li, Y., Pöschl, U., and Shiraiwa, M.: Molecular corridors and parameterizations of volatility in  
702 the chemical evolution of organic aerosols, *Atmos. Chem. Phys.*, 16, 3327-3344, 2016.

703 Li, Y. J., Liu, P., Gong, Z., Wang, Y., Bateman, A. P., Bergoend, C., Bertram, A. K., and Martin,  
704 S. T.: Chemical Reactivity and Liquid/Nonliquid States of Secondary Organic Material, *Environ.*  
705 *Sci. Technol.*, 49, 13264-13274, 2015.

706 Lienhard, D. M., Huisman, A. J., Krieger, U. K., et al.: Viscous organic aerosol particles in the  
707 upper troposphere: diffusivity-controlled water uptake and ice nucleation?, *Atmos. Chem. Phys.*,  
708 15, 13599-13613, 2015.

709 Lignell, H., Hinks, M. L., and Nizkorodov, S. A.: Exploring matrix effects on photochemistry of  
710 organic aerosols, *Proc. Natl. Acad. Sci. U.S.A.*, 111, 13780-13785, 2014.

711 Liu, P., Li, Y. J., Wang, Y., Gilles, M. K., Zaveri, R. A., Bertram, A. K., and Martin, S. T.:  
712 Lability of secondary organic particulate matter, *Proc. Natl. Acad. Sci. U.S.A.*, 113, 12643-  
713 12648, 2016.

714 Liu, P., Li, Y. J., Wang, Y., Bateman, A. P., Zhang, Y., Gong, Z., Bertram, A. K., and Martin, S.  
715 T.: Highly Viscous States Affect the Browning of Atmospheric Organic Particulate Matter, *ACS*  
716 *Central Science*, 4, 207-215, 2018.

717 Loza, C. L., Coggon, M. M., Nguyen, T. B., Zuend, A., Flagan, R. C., and Seinfeld, J. H.: On the  
718 mixing and evaporation of secondary organic aerosol components, *Environ. Sci. Technol.*, 47,  
719 6173-6180, 2013.

720 Maclean, A. M., Butenhoff, C. L., Grayson, J. W., Barsanti, K., Jimenez, J. L., and Bertram, A.  
721 K.: Mixing times of organic molecules within secondary organic aerosol particles: a global  
722 planetary boundary layer perspective, *Atmos. Chem. Phys.*, 17, 13037-13048, 2017.

723 Mai, H., Shiraiwa, M., Flagan, R. C., and Seinfeld, J. H.: Under What Conditions Can  
724 Equilibrium Gas-Particle Partitioning Be Expected to Hold in the Atmosphere?, *Environ. Sci.*  
725 *Technol.*, 49, 11485-11491, 2015.

- 726 Marshall, F. H., Miles, R. E. H., Song, Y.-C., Ohm, P. B., Power, R. M., Reid, J. P., and Dutcher,  
727 C. S.: Diffusion and reactivity in ultraviscous aerosol and the correlation with particle viscosity,  
728 Chem. Sci., 7, 1298-1308, 2016.
- 729 Matsushima, S., Takano, A., Takahashi, Y., and Matsushita, Y.: Precise synthesis of a series of  
730 poly(4-n-alkylstyrene)s and their glass transition temperatures, Journal of Polymer Science Part  
731 B: Polymer Physics, 55, 757-763, 2017.
- 732 Metatla, N., and Soldera, A.: The Vogel– Fulcher– Tamman Equation Investigated by Atomistic  
733 Simulation with Regard to the Adam– Gibbs Model, Macromolecules, 40, 9680-9685, 2007.
- 734 Mikhailov, E., Vlasenko, S., Martin, S. T., Koop, T., and Pöschl, U.: Amorphous and crystalline  
735 aerosol particles interacting with water vapor: conceptual framework and experimental evidence  
736 for restructuring, phase transitions and kinetic limitations, Atmos. Chem. Phys., 9, 9491-9522,  
737 2009.
- 738 Montserrat, S., and Colomer, P.: The effect of the molecular weight on the glass transition  
739 temperature in amorphous poly(ethylene terephthalate), Polymer Bulletin, 12, 173-180, 1984.
- 740 Murray, B. J., Wilson, T. W., Dobbie, S., et al.: Heterogeneous nucleation of ice particles on  
741 glassy aerosols under cirrus conditions, Nat. Geosci., 3, 233-237, 2010.
- 742 Nakanishi, M., and Nozaki, R.: Systematic study of the glass transition in polyhydric alcohols,  
743 Physical Review E, 83, 051503, 2011.
- 744 Nguyen, T. B., Nizkorodov, S. A., Laskin, A., and Laskin, J.: An approach toward quantification  
745 of organic compounds in complex environmental samples using high-resolution electrospray  
746 ionization mass spectrometry, Anal. Methods, 5, 72-80, 2013.
- 747 Nizkorodov, S. A., Laskin, J., and Laskin, A.: Molecular chemistry of organic aerosols through  
748 the application of high resolution mass spectrometry, Phys. Chem. Chem. Phys., 13, 3612-3629,  
749 2011.
- 750 Nozière, B., Kalberer, M., Claeys, M., et al.: The Molecular Identification of Organic  
751 Compounds in the Atmosphere: State of the Art and Challenges, Chem. Rev., 115, 3919–3983,  
752 2015.
- 753 O’Connell, P. A., and McKenna, G. B.: Arrhenius-type temperature dependence of the segmental  
754 relaxation below  $T_g$ , J. Chem. Phys., 110, 11054-11060, 1999.
- 755 Onder, K., Peters, R. H., and Spark, L. C.: Melting and transition phenomena in some polyester-  
756 urethanes, Polymer, 13, 133-139, 1972.
- 757 Pajunoja, A., Malila, J., Hao, L., Joutsensaari, J., Lehtinen, K. E. J., and Virtanen, A.: Estimating  
758 the viscosity range of SOA particles based on their coalescence time, Aerosol Sci. Technol., 48,  
759 i-iv, 2014.

- 760 Pajunoja, A., Lambe, A. T., Hakala, J., et al.: Adsorptive uptake of water by semisolid secondary  
761 organic aerosols, *Geophys. Res. Lett.*, 42, 3063-3068, 2015.
- 762 Papadopoulos, P., Floudas, G., Chi, C., and Wegner, G.: Molecular dynamics of oligofluorenes:  
763 A dielectric spectroscopy investigation, *J. Chem. Phys.*, 120, 2368-2374, 2004.
- 764 Perraud, V., Bruns, E. A., Ezell, M. J., et al.: Nonequilibrium atmospheric secondary organic  
765 aerosol formation and growth, *Proc. Natl. Acad. Sci. U.S.A.*, 109, 2836-2841, 2012.
- 766 Petters, M. D., and Kreidenweis, S. M.: A single parameter representation of hygroscopic growth  
767 and cloud condensation nucleus activity, *Atmos. Chem. Phys.*, 7, 1961-1971, 2007.
- 768 Petters, S. S., Pagonis, D., Claflin, M. S., Levin, E. J. T., Petters, M. D., Ziemann, P. J., and  
769 Kreidenweis, S. M.: Hygroscopicity of Organic Compounds as a Function of Carbon Chain  
770 Length and Carboxyl, Hydroperoxy, and Carbonyl Functional Groups, *J. Phys. Chem. A*, 121,  
771 5164-5174, 2017.
- 772 *Polymer handbook*, t. e.: J. Brandrup (Editor), Edmund H. Immergut (Editor), E. A. Grulke  
773 (Editor), John Wiley & Sons, Inc., ISBN 0-471-16628-6, 1999.
- 774 Pratap, V., Chen, Y., Yao, G., and Nakao, S.: Temperature effects on multiphase reactions of  
775 organic molecular markers: A modeling study, *Atmos. Environ.*, 179, 40-48, 2018.
- 776 Price, H. C., Murray, B. J., Mattsson, J., O'Sullivan, D., Wilson, T. W., Baustian, K. J., and  
777 Benning, L. G.: Quantifying water diffusion in high-viscosity and glassy aqueous solutions using  
778 a Raman isotope tracer method, *Atmos. Chem. Phys.*, 14, 3817-3830, 2014.
- 779 Putman, A. L., Offenberg, J. H., Fisseha, R., Kundu, S., Rahn, T. A., and Mazzoleni, L. R.:  
780 Ultrahigh-resolution FT-ICR mass spectrometry characterization of  $\alpha$ -pinene ozonolysis SOA,  
781 *Atmos. Environ.*, 46, 164-172, 2012.
- 782 Raffaelli, A., and Saba, A.: Atmospheric pressure photoionization mass spectrometry, *Mass  
783 Spectrom. Rev.*, 22, 318-331, 2003.
- 784 Reid, J. P., Bertram, A. K., Topping, D. O., Laskin, A., Martin, S. T., Petters, M. D., Pope, F. D.,  
785 and Rovelli, G.: The viscosity of atmospherically relevant organic particles, *Nat. Commun.*, 9,  
786 956, 2018.
- 787 Renbaum-Wolff, L., Grayson, J. W., Bateman, A. P., Kuwata, K., Sellier, M., Murray, B. J.,  
788 Schilling, J. E., Martin, S. T., and Bertram, A. K.: Viscosity of  $\alpha$ -pinene secondary organic  
789 material and implications for particle growth and reactivity, *Proc. Natl. Acad. Sci. U.S.A.*, 110,  
790 8014-8019, 2013.
- 791 Roach, P. J., Laskin, J., and Laskin, A.: Nanospray desorption electrospray ionization: an  
792 ambient method for liquid-extraction surface sampling in mass spectrometry, *Analyst*  
793 (Cambridge, U. K.), 135, 2233-2236, 2010a.

- 794 Roach, P. J., Laskin, J., and Laskin, A.: Molecular Characterization of Organic Aerosols Using  
795 Nanospray-Desorption/Electrospray Ionization-Mass Spectrometry, *Anal. Chem.* (Washington,  
796 DC, U. S.), 82, 7979-7986, 2010b.
- 797 Roldin, P., Eriksson, A. C., Nordin, E. Z., et al.: Modelling non-equilibrium secondary organic  
798 aerosol formation and evaporation with the aerosol dynamics, gas- and particle-phase chemistry  
799 kinetic multilayer model ADCHAM, *Atmos. Chem. Phys.*, 14, 7953-7993, 2014.
- 800 Roos, Y.: Melting and glass transitions of low molecular weight carbohydrates, *Carbohydr. Res.*,  
801 238, 39-48, 1993.
- 802 Rothfuss, N. E., and Petters, M. D.: Influence of Functional Groups on the Viscosity of Organic  
803 Aerosol, *Environ. Sci. Technol.*, 51, 271-279, 2017.
- 804 Sastri, S. R. S., and Rao, K. K.: A new group contribution method for predicting viscosity of  
805 organic liquids, *The Chemical Engineering Journal*, 50, 9-25, 1992.
- 806 Saukko, E., Lambe, A. T., Massoli, P., et al.: Humidity-dependent phase state of SOA particles  
807 from biogenic and anthropogenic precursors, *Atmos. Chem. Phys.*, 12, 7517-7529, 2012.
- 808 Schill, G. P., and Tolbert, M. A.: Heterogeneous ice nucleation on phase-separated organic-  
809 sulfate particles: effect of liquid vs. glassy coatings, *Atmos. Chem. Phys.*, 13, 4681-4695, 2013.
- 810 Schill, G. P., De Haan, D. O., and Tolbert, M. A.: Heterogeneous Ice Nucleation on Simulated  
811 Secondary Organic Aerosol, *Environ. Sci. Technol.*, 48, 1675-1682, 2014.
- 812 Selimovic, V., Yokelson, R. J., Warneke, C., Roberts, J. M., de Gouw, J., Reardon, J., and  
813 Griffith, D. W. T.: Aerosol optical properties and trace gas emissions by PAX and OP-FTIR for  
814 laboratory-simulated western US wildfires during FIREX, *Atmos. Chem. Phys. Discuss.*, 2017,  
815 1-34, 2017.
- 816 Shiraiwa, M., Ammann, M., Koop, T., and Pöschl, U.: Gas uptake and chemical aging of  
817 semisolid organic aerosol particles, *Proc. Natl. Acad. Sci. U.S.A.*, 108, 11003-11008, 2011.
- 818 Shiraiwa, M., and Seinfeld, J. H.: Equilibration timescale of atmospheric secondary organic  
819 aerosol partitioning, *Geophys. Res. Lett.*, 39, L24801, 2012.
- 820 Shiraiwa, M., Yee, L. D., Schilling, K. A., Loza, C. L., Craven, J. S., Zuend, A., Ziemann, P. J.,  
821 and Seinfeld, J. H.: Size distribution dynamics reveal particle-phase chemistry in organic aerosol  
822 formation, *Proc. Natl. Acad. Sci. U.S.A.*, 110, 11746-11750, 2013.
- 823 Shiraiwa, M., Berkemeier, T., Schilling-Fahnestock, K. A., Seinfeld, J. H., and Pöschl, U.:  
824 Molecular corridors and kinetic regimes in the multiphase chemical evolution of secondary  
825 organic aerosol, *Atmos. Chem. Phys.*, 14, 8323-8341, 2014.
- 826 Shiraiwa, M., Li, Y., Tsimpidi, A. P., Karydis, V. A., Berkemeier, T., Pandis, S. N., Lelieveld, J.,  
827 Koop, T., and Pöschl, U.: Global distribution of particle phase state in atmospheric secondary  
828 organic aerosols, *Nat. Commun.*, 8, 15002, 2017.

- 829 Shrivastava, M., Cappa, C. D., Fan, J., et al.: Recent advances in understanding secondary  
830 organic aerosol: Implications for global climate forcing, *Rev. Geophys.*, 55, 509-559, 2017.
- 831 Slade, J. H., and Knopf, D. A.: Multiphase OH Oxidation Kinetics of Organic Aerosol: The Role  
832 of Particle Phase State and Relative Humidity, *Geophys. Res. Lett.*, 2014GL060582, 2014.
- 833 Song, M., Liu, P. F., Hanna, S. J., Li, Y. J., Martin, S. T., and Bertram, A. K.: Relative humidity-  
834 dependent viscosities of isoprene-derived secondary organic material and atmospheric  
835 implications for isoprene-dominant forests, *Atmos. Chem. Phys.*, 15, 5145-5159, 2015.
- 836 Song, M., Liu, P. F., Hanna, S. J., Zaveri, R. A., Potter, K., You, Y., Martin, S. T., and Bertram,  
837 A. K.: Relative humidity-dependent viscosity of secondary organic material from toluene photo-  
838 oxidation and possible implications for organic particulate matter over megacities, *Atmos. Chem.*  
839 *Phys.*, 16, 8817-8830, 2016a.
- 840 Song, Y. C., Haddrell, A. E., Bzdek, B. R., Reid, J. P., Bannan, T., Topping, D. O., Percival, C.,  
841 and Cai, C.: Measurements and Predictions of Binary Component Aerosol Particle Viscosity, *J.*  
842 *Phys. Chem. A*, 120, 8123-8137, 2016b.
- 843 Tolocka, M. P., Jang, M., Ginter, J. M., Cox, F. J., Kamens, R. M., and Johnston, M. V.:  
844 Formation of oligomers in secondary organic aerosol, *Environ. Sci. Technol.*, 38, 1428-1434,  
845 2004.
- 846 US-EPA: Estimation programs interface suite for microsoft windows, 2012.
- 847 Vaden, T. D., Imre, D., Beranek, J., Shrivastava, M., and Zelenyuk, A.: Evaporation kinetics and  
848 phase of laboratory and ambient secondary organic aerosol, *Proc. Natl. Acad. Sci. U.S.A.*, 108,  
849 2190-2195, 2011.
- 850 van der Sman, R. G. M.: Predictions of Glass Transition Temperature for Hydrogen Bonding  
851 Biomaterials, *J. Phys. Chem. B*, 117, 16303-16313, 2013.
- 852 Virtanen, A., Joutsensaari, J., Koop, T., et al.: An amorphous solid state of biogenic secondary  
853 organic aerosol particles, *Nature*, 467, 824-827, 2010.
- 854 Wang, B., O'Brien, R. E., Kelly, S. T., Shilling, J. E., Moffet, R. C., Gilles, M. K., and Laskin,  
855 A.: Reactivity of Liquid and Semisolid Secondary Organic Carbon with Chloride and Nitrate in  
856 Atmospheric Aerosols, *J. Phys. Chem. A*, 119, 4498-4508, 2015.
- 857 Wang, B. B., Lambe, A. T., Massoli, P., Onasch, T. B., Davidovits, P., Worsnop, D. R., and  
858 Knopf, D. A.: The deposition ice nucleation and immersion freezing potential of amorphous  
859 secondary organic aerosol: Pathways for ice and mixed-phase cloud formation, *J. Geophys. Res.-*  
860 *Atmos.*, 117, D16209, 2012a.
- 861 Wang, B. B., Laskin, A., Roedel, T., Gilles, M. K., Moffet, R. C., Tivanski, A. V., and Knopf, D.  
862 A.: Heterogeneous ice nucleation and water uptake by field-collected atmospheric particles  
863 below 273 K, *J. Geophys. Res.-Atmos.*, 117, D00v19, 2012b.

- 864 White, R. P., and Lipson, J. E. G.: Polymer free volume and its connection to the glass transition,  
865 *Macromolecules*, 49, 3987-4007, 2016.
- 866 Williams, M. L., Landel, R. F., and Ferry, J. D.: The temperature dependence of relaxation  
867 mechanisms in amorphous polymers and other glass-forming liquids, *J. Am. Chem. Soc.*, 77,  
868 3701-3707, 1955.
- 869 Ye, Q., Robinson, E. S., Ding, X., Ye, P., Sullivan, R. C., and Donahue, N. M.: Mixing of  
870 secondary organic aerosols versus relative humidity, *Proc. Natl. Acad. Sci. U.S.A.*, 113, 12649-  
871 12654, 2016.
- 872 Ye, Q., Upshur, M. A., Robinson, E. S., Geiger, F. M., Sullivan, R. C., Thomson, R. J., and  
873 Donahue, N. M.: Following Particle-Particle Mixing in Atmospheric Secondary Organic  
874 Aerosols by Using Isotopically Labeled Terpenes, *Chem*, 4, 318-333, 2018.
- 875 Yli-Juuti, T., Pajunoja, A., Tikkanen, O.-P., et al.: Factors controlling the evaporation of  
876 secondary organic aerosol from  $\alpha$ -pinene ozonolysis, *Geophys. Res. Lett.*, 44, 2562-2570, 2017.
- 877 You, Y., Smith, M. L., Song, M., Martin, S. T., and Bertram, A. K.: Liquid-liquid phase  
878 separation in atmospherically relevant particles consisting of organic species and inorganic salts,  
879 *Int. Rev. Phys. Chem.*, 33, 43-77, 2014.
- 880 Zaveri, R. A., Easter, R. C., Shilling, J. E., and Seinfeld, J. H.: Modeling kinetic partitioning of  
881 secondary organic aerosol and size distribution dynamics: representing effects of volatility, phase  
882 state, and particle-phase reaction, *Atmos. Chem. Phys.*, 14, 5153-5181, 2014.
- 883 Zaveri, R. A., Shilling, J. E., Zelenyuk, A., et al.: Growth Kinetics and Size Distribution  
884 Dynamics of Viscous Secondary Organic Aerosol, *Environ. Sci. Technol.*, 52, 1191-1199, 2018.
- 885 Zhang, Y., Sanchez, M. S., Douet, C., et al.: Changing shapes and implied viscosities of  
886 suspended submicron particles, *Atmos. Chem. Phys.*, 15, 7819-7829, 2015.
- 887 Zhang, Y., Chen, Y., Lambe, A. T., et al.: Effect of the Aerosol-Phase State on Secondary  
888 Organic Aerosol Formation from the Reactive Uptake of Isoprene-Derived Epoxydiols (IEPOX),  
889 *Environ. Sci. Technol. Lett.*, 2018.
- 890 Zhou, S., Shiraiwa, M., McWhinney, R., Pöschl, U., and Abbatt, J. P. D.: Kinetic limitations in  
891 gas-particle reactions arising from slow diffusion in secondary organic aerosol, *Faraday Discuss.*,  
892 165, 391-406, 2013.
- 893 Zobrist, B., Marcolli, C., Pedernera, D. A., and Koop, T.: Do atmospheric aerosols form  
894 glasses?, *Atmos. Chem. Phys.*, 8, 5221-5244, 2008.
- 895 Zobrist, B., Soonsin, V., Luo, B. P., Krieger, U. K., Marcolli, C., Peter, T., and Koop, T.: Ultra-  
896 slow water diffusion in aqueous sucrose glasses, *Phys. Chem. Chem. Phys.*, 13, 3514-3526,  
897 2011.
- 898
- 899

900 **Table 1.** Composition classes and the  $n_C^0$  and  $b$  values (K) for glass transition temperature  
 901 parameterizations obtained by least-squares optimization using the measurements compiled in  
 902 Koop et al., (2011), Dette et al., (2014) and Rothfuss and Petters (2017).

Classes	$n_C^0$	$b_C$	$b_H$	$b_{CH}$	$b_O$	$b_{CO}$
CH	1.96 (±1.81)	61.99 (±53.65)	-113.33 (±44.47)	28.74 (±20.86)		
CHO	12.13 (±2.66)	10.95 (±13.60)	-41.82 (±14.78)	21.61 (±5.30)	118.96 (±9.72)	-24.38 (±4.21)

903

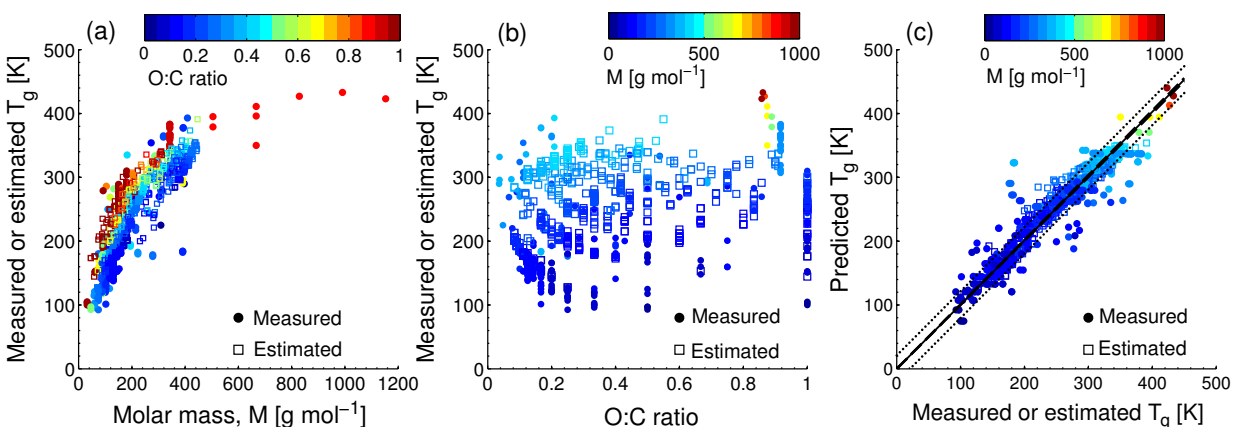
904

905

906 **Table 2.** Glass transition temperatures calculated using Eq. (1) and (2) for toluene SOA mixtures  
 907 at low relative humidity (low RH < 2%) and high relative humidity (high RH = 75%) conditions.

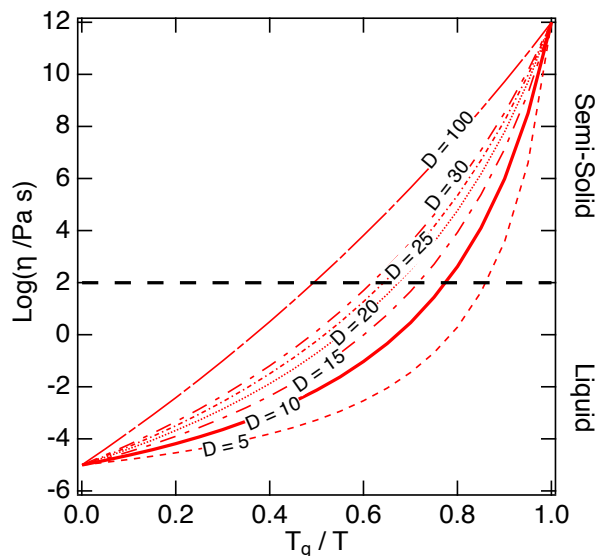
$T_{g,org}$ (K)	low RH	high RH
Equation (1)*	299	295
Equation (2)	313	303

908 \* Compounds with  $M > 450$  g mol<sup>-1</sup> were excluded from the analysis.



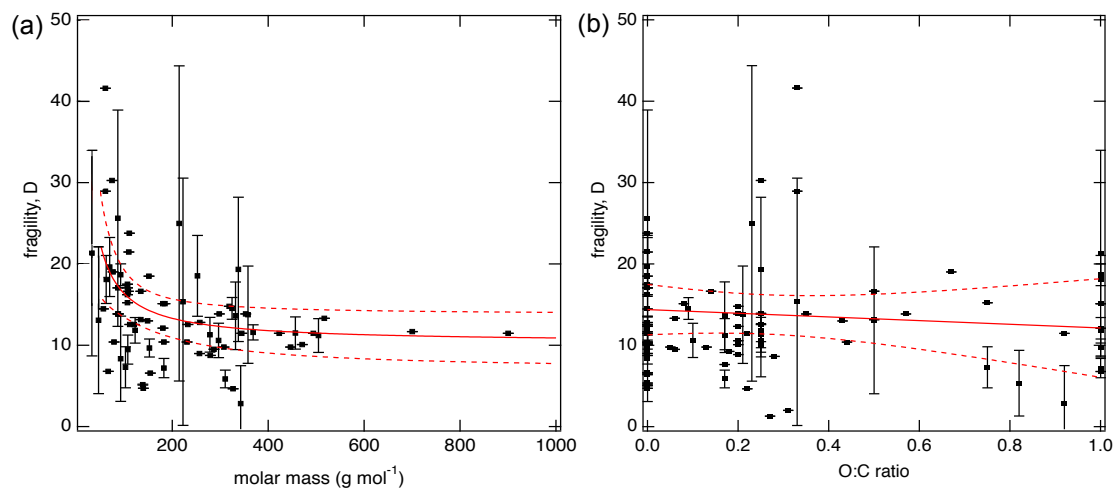
909  
 910 **Figure 1.** Characteristic relationships between molecular properties and the glass transition  
 911 temperature ( $T_g$ ) of organic compounds. (a)  $T_g$  of organic compounds as measured (circles) and  
 912 estimated with the Boyer-Kauzmann rule (squares) plotted against molar mass. The markers are  
 913 color-coded by atomic O:C ratio. (b) Measured (circles) and estimated (squares)  $T_g$  of organic  
 914 compounds plotted against O:C ratio. The markers are color-coded by molar mass. (c) Predicted  
 915  $T_g$  for CHO compounds using a parameterization (Eq. 2) developed in this study compared to  
 916 measured (circles) and estimated  $T_g$  by the Boyer-Kauzmann rule (squares). The solid line shows  
 917 1:1 line and the dashed and dotted lines show 68% confidence and prediction bands,  
 918 respectively.

919  
 920

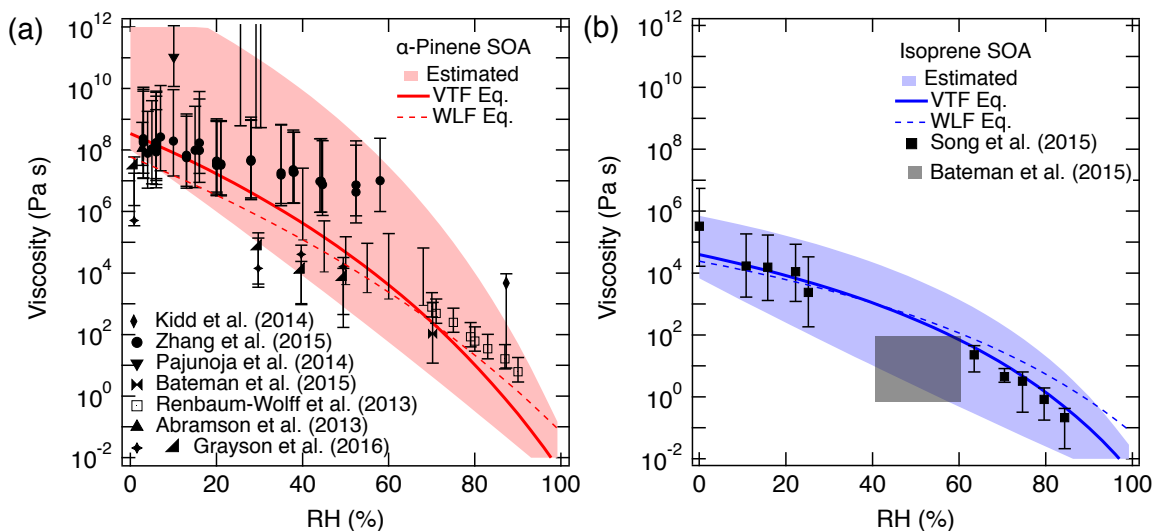


921  
 922 **Figure 2.** The Angell plot of viscosity ( $\eta$ ) vs.  $T_g/T$ . The lines represent different fragility  
 923 parameter ( $D$ ) values in the range of 5 - 100, with  $D = 10$  (the solid line) used as a base case for  
 924 this study. A large fragility parameter value is associated with a strong glass former, while  
 925 fragile materials are associated with lower values. The black dashed line at viscosity of  $10^2$  Pa s  
 926 indicates the approximate threshold between liquid and semi-solid states.

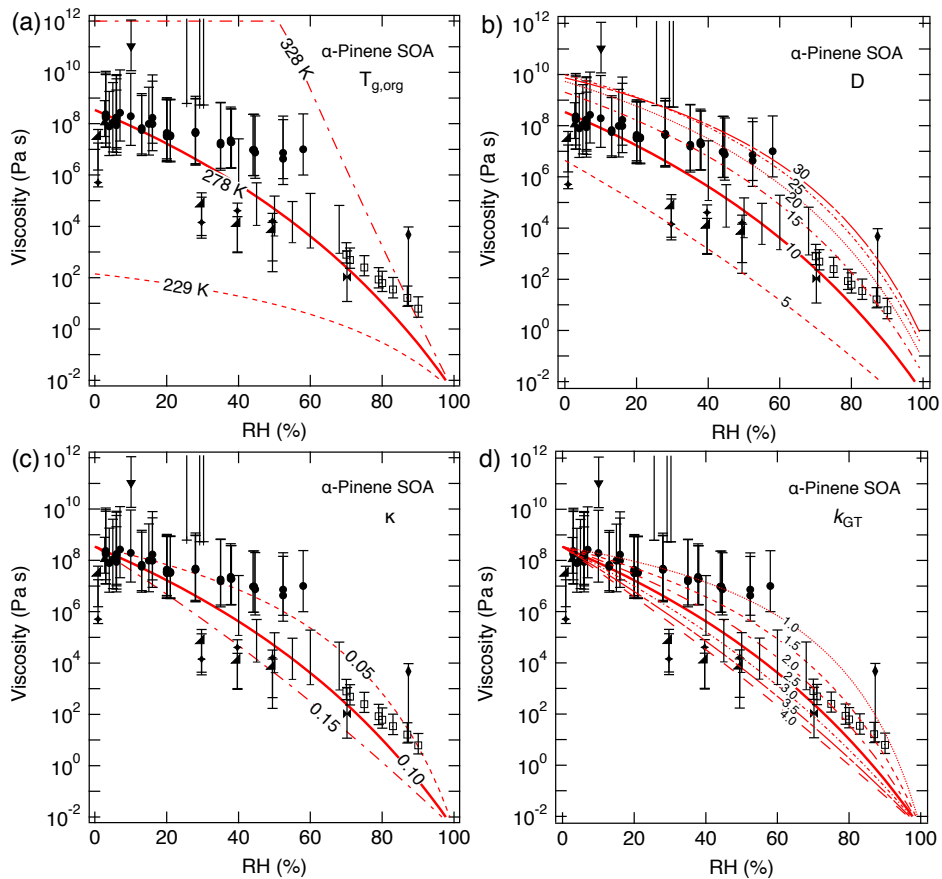




927  
 928 **Figure 3.** Fragility parameter of organic compounds ( $D$ ) plotted against (a) molar mass and (b)  
 929 atomic O:C ratio. Error bars are standard deviations. The solid red lines represent the fitted  
 930 curves with fitted equations for (a)  $D = 602.6/M + 10.3$  and (b)  $D = 14.4 - 2.3(\text{O:C})$  respectively.  
 931 Dashed red lines indicate the 95% confidence band.  
 932  
 933

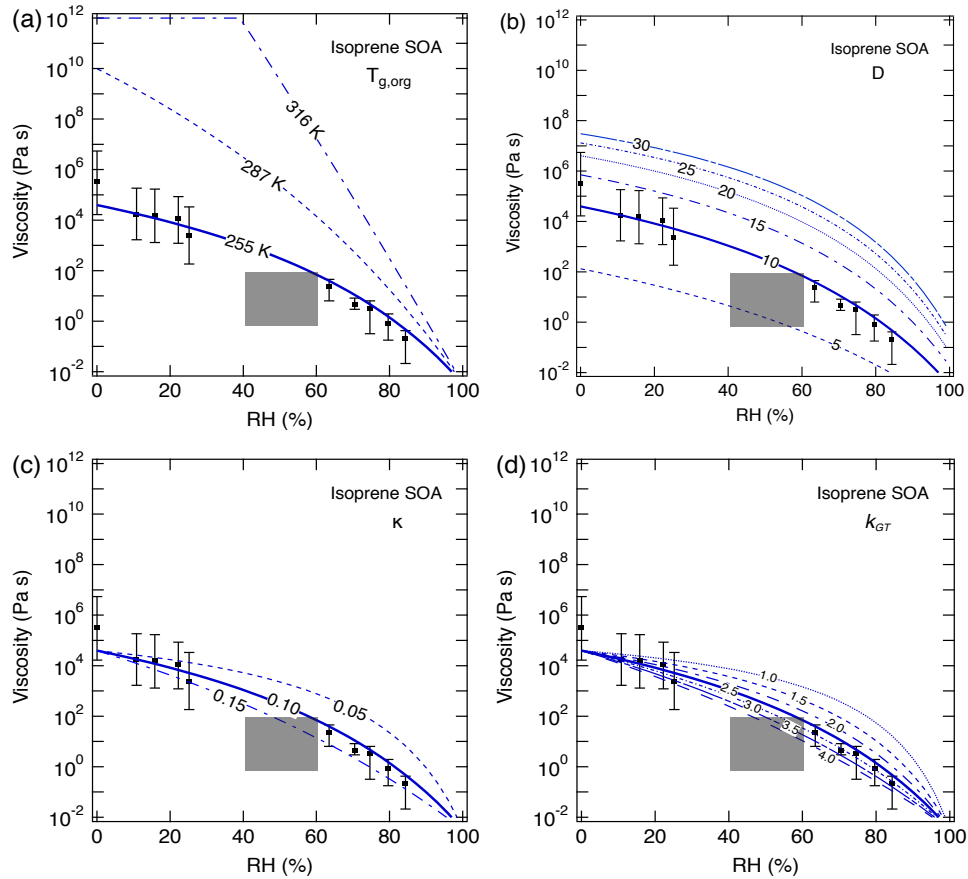


934  
 935 **Figure 4.** Comparison of measured and predicted viscosity of (a)  $\alpha$ -pinene SOA and (b) isoprene  
 936 SOA at 295 K as a function of RH. The solid lines represent base simulations with the VTF  
 937 equation, while the dotted line represents viscosity predicted using the WLF equation  
 938 [parameters: glass transition temperature of dry SOA ( $T_{g,org}$ ), fragility ( $D$ ), hygroscopicity ( $\kappa$ )  
 939 and Gordon-Taylor constant ( $k_{GT}$ ): (a) 278.5 K, 0.1, 10 and 2.5; (b) 255 K, 0.1, 10 and 2.5. The  
 940 shaded regions were determined by varying these parameters (a) upper (lower) limit:  $T_{g,org}$  = 300  
 941 K (278.5 K),  $\kappa$  = 0.1 (0.1),  $D$  = 20 (10),  $k_{GT}$  = 2.5 (2.0); (b) upper (lower limit):  $T_{g,org}$  = 255 K  
 942 (255 K),  $\kappa$  = 0.10 (0.15),  $D$  = 15 (8),  $k_{GT}$  = 2.5 (4.0). **Panel (a):** Renbaum-Wolff et al. (2013) data  
 943 represents viscosity for water-soluble portion of SOA; Grayson et al. (2016) data in the panel (a)  
 944 represents two different mass loadings ( $121 \mu\text{g m}^{-3}$ ;  $520 \mu\text{g m}^{-3}$ ). **Panel (b):** The gray box in  
 945 panel (b) represents estimated viscosity based on bounce measurements of Bateman et al. (2015).  
 946



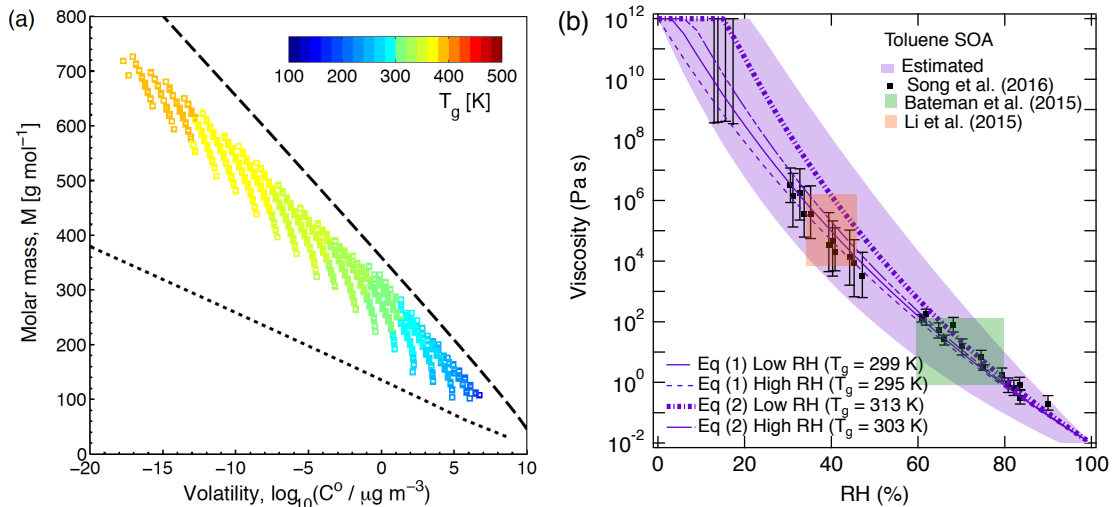
947  
948

949 **Figure 5.** Sensitivity calculations for viscosity of  $\alpha$ -pinene SOA at 295 K as a function of RH by  
 950 varying: (a) glass transition temperature of dry SOA ( $T_{g,org}$ ), (b) fragility ( $D$ ), (c) hygroscopicity  
 951 ( $\kappa$ ), and (d) Gordon-Taylor constant ( $k_{GT}$ ).



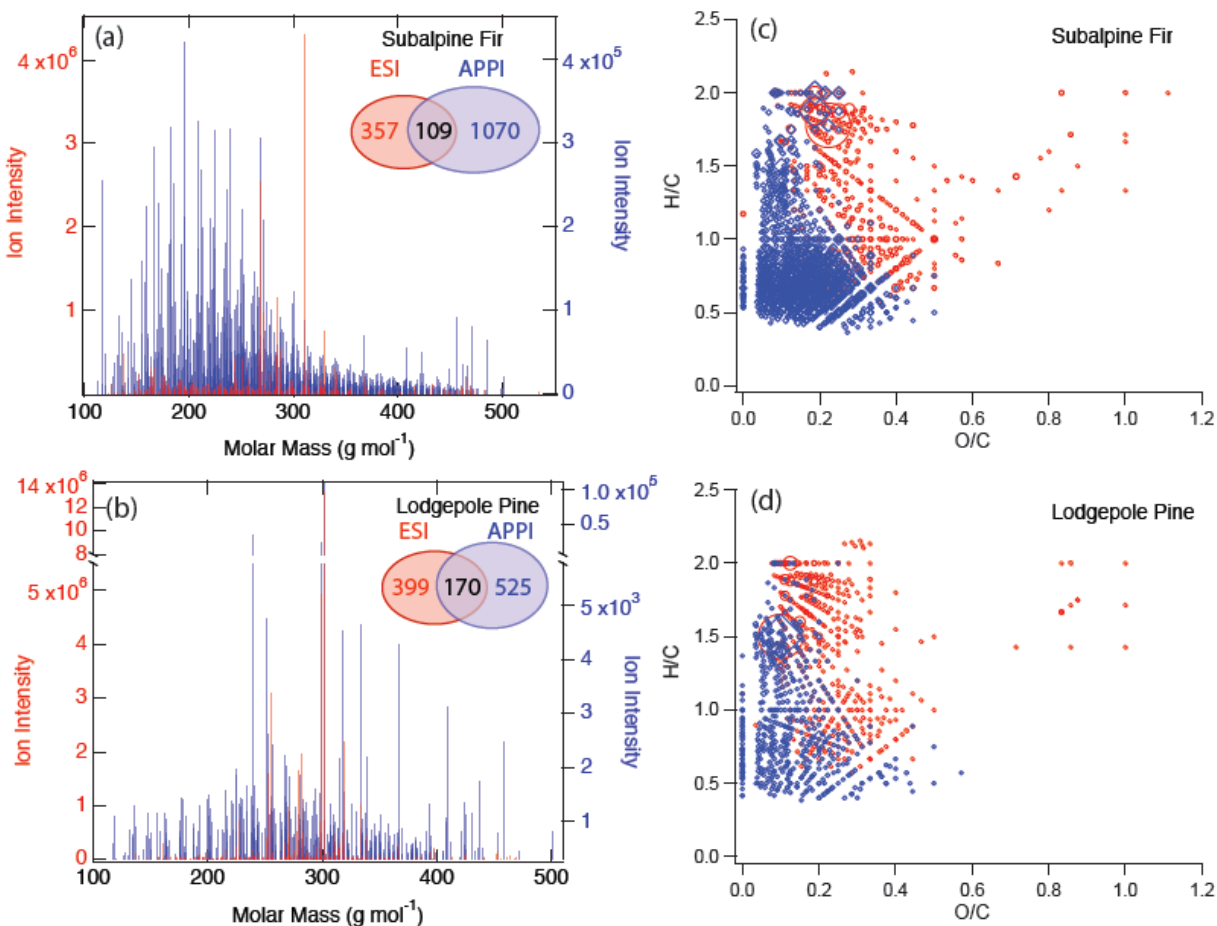
952  
 953  
 954  
 955  
 956  
 957  
 958  
 959

**Figure 6.** Sensitivity calculations for viscosity of isoprene SOA at 295 K as a function of RH by varying: (a) glass transition temperature of dry SOA ( $T_{g,org}$ ), (b) fragility ( $D$ ), (c) hygroscopicity ( $\kappa$ ), and (d) Gordon-Taylor constant ( $k_{GT}$ ). Data points are measured viscosity by Song et al. (2015) and the gray box represents estimated viscosity based on bounce measurements of Bateman et al. (2015).

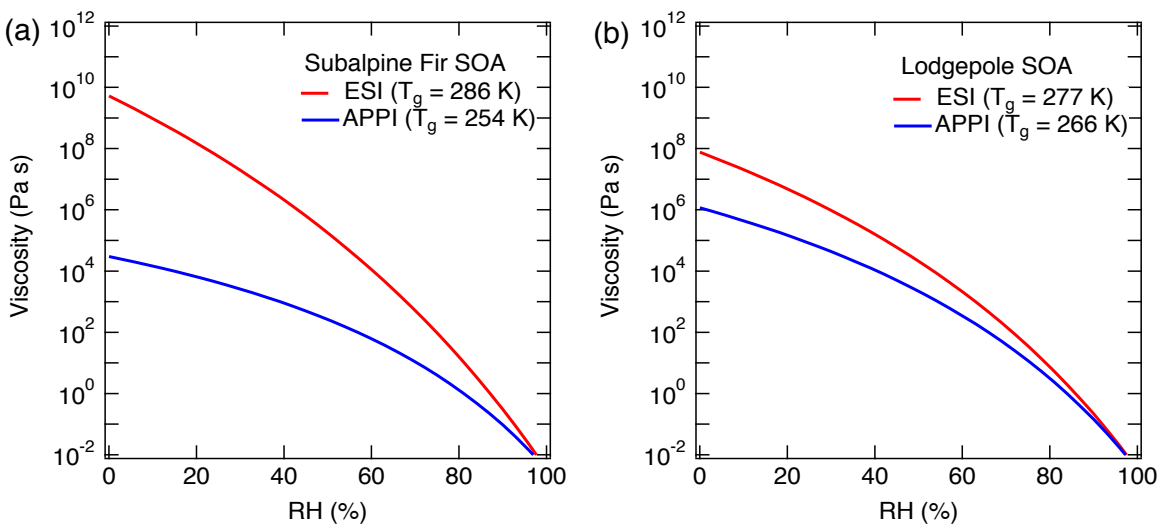


960

961 **Figure 7.** (a) Molecular corridor of molar mass plotted against volatility of toluene SOA formed  
 962 under dry conditions (Hinks et al., 2017) color-coded by glass transition temperature ( $T_g$ )  
 963 estimated using Eq. (2). The upper dashed line indicates the low O:C bound of the molecular  
 964 corridor (linear alkanes  $C_nH_{2n+2}$  with O:C = 0), and the lower dotted line indicates the high O:C  
 965 bound (sugar alcohols  $C_nH_{2n+2}O_n$  with O:C = 1). (b) Comparison of measured (markers) and  
 966 modeled (lines) viscosity of toluene SOA at 295 K as a function of RH. Viscosities were  
 967 calculated using fragility ( $D$ ) of 13, the hygroscopicity ( $\kappa$ ) of 0.25 and the Gordon-Taylor  
 968 constant ( $k_{GT}$ ) of 3.0 with different glass transition temperatures of dry SOA ( $T_{g,org}$ ) as estimated  
 969 using Eq. (1) or (2) under low and high RH conditions. The shaded regions were calculated by  
 970 varying those parameters:  $T_{g,org} = 313$  K (295 K),  $\kappa = 0.20$  (0.25),  $D = 13$  (10),  $k_{GT} = 2.5$  (3.5) for  
 971 the upper (lower) limit. Mass loadings were  $23 \mu\text{g m}^{-3}$  for LRH and  $8 \mu\text{g m}^{-3}$  for HRH (Hinks et  
 972 al., 2017).  
 973

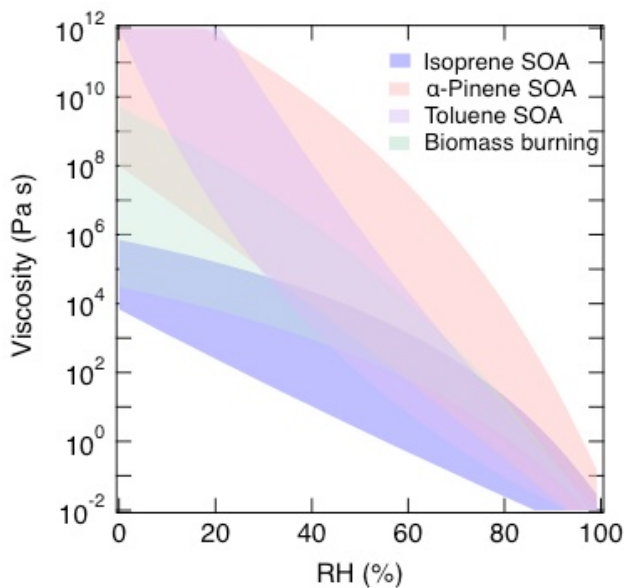


974  
 975 **Figure 8.** Mass spectra of biomass burning organic particles collected from test burns of (a)  
 976 subalpine fir and (b) lodgepole pine as measured by high resolution mass spectrometry with  
 977 two ionization techniques: electron spray ionization (ESI, red) and atmospheric pressure  
 978 photoionization (APPI; blue). Numbers of elemental formulas identified by ESI (red), APPI  
 979 (blue) and both modes (black) are also specified. Van Krevelen plots of the compounds  
 980 identified by ESI (red) and APPI (blue) mode in BBOA from burning of (c) subalpine fir and (d)  
 981 lodgepole pine.  
 982

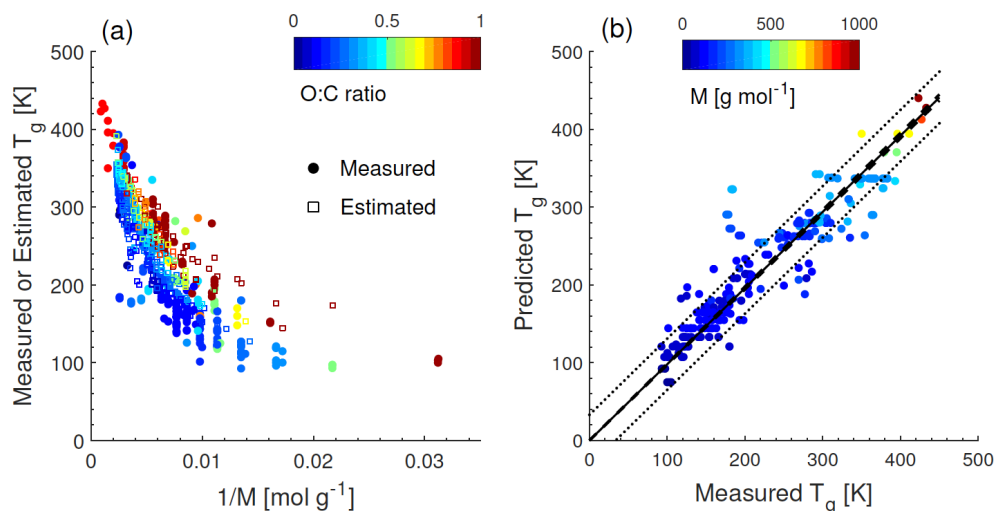


983  
 984 **Figure 9.** Predicted viscosity for biomass burning particles of (a) subalpine fir and (b) lodgepole  
 985 pine trees as measured by high resolution mass spectrometry with two ionization techniques:  
 986 electro spray ionization (ESI, red) and atmospheric pressure photoionization (APPI; blue).  $T_{g,org}$   
 987 are specified in the figure legend and other used parameters are fixed to  $\kappa = 0.1$ ,  $D = 10$ ,  $k_{GT} =$   
 988 2.5.

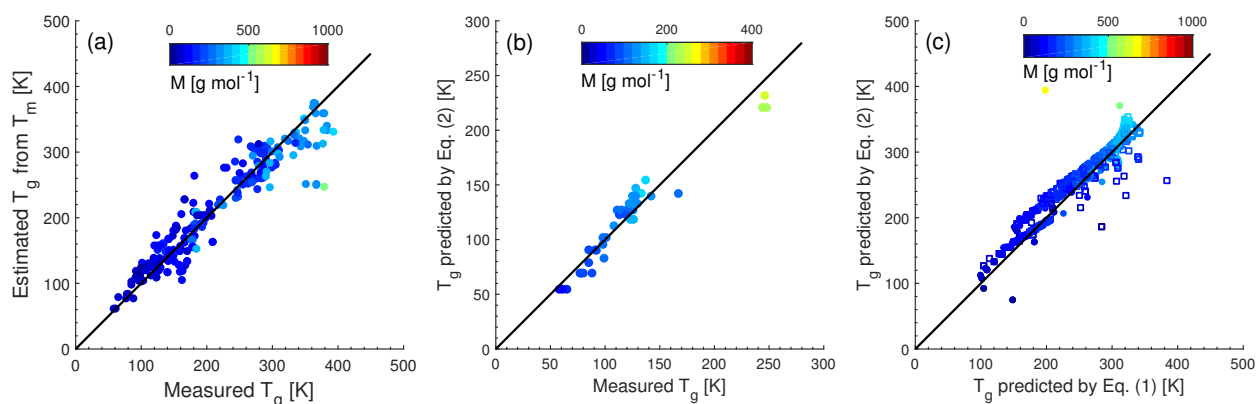
989  
 990  
 991  
 992



993  
 994 **Figure 10.** Summary of predicted range of viscosity of  $\alpha$ -pinene SOA (red), isoprene SOA  
 995 (blue), toluene SOA (purple), and biomass burning particles (green).  
 996

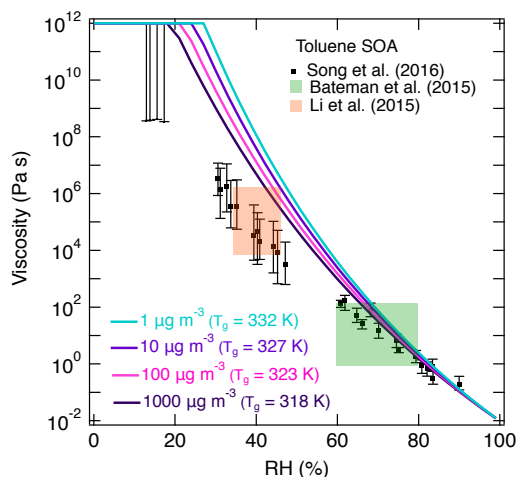


997  
 998 **Figure A1.** (a)  $T_g$  of organic compounds as measured (circles) and estimated with the Boyer-  
 999 Kauszmann rule (squares) plotted against the inverse molar mass. The markers are color-coded by  
 1000 atomic O:C ratio. (b) Predicted  $T_g$  for CHO compounds using a parameterization (Eq. 2)  
 1001 developed in this study compared to measured  $T_g$  (circles). The solid line shows 1:1 line and the  
 1002 dashed and dotted lines show 68% confidence and prediction bands, respectively.  
 1003



1004  
 1005 **Figure A2.** (a) Comparison of measured and estimated  $T_g$  by the Boyer-Kauszmann rule for 251  
 1006 organic compounds (Koop et al., 2011; Dette et al., 2014; Rothfuss and Petters 2017) with their  
 1007 measured  $T_m$  available. The markers are color-coded by molar mass. (b, c) Predicted  $T_g$  using Eq.  
 1008 (2) compared with (b) measured  $T_g$  for CH compounds and (c) predicted  $T_g$  using Eq. (1) for  
 1009 CHO compounds. The solid line shows 1:1 line. Solid circle markers represent organic  
 1010 compounds as compiled in Koop et al. (2011) and open square marker represent SOA oxidation  
 1011 products in Shiraiwa et al. (2014) in panel (c).  
 1012





1013  
 1014 **Figure A3.** Effect of mass loading on predicted viscosity for toluene SOA. Solid lines represent  
 1015 the predicted viscosity with Eq. (2) using chemical composition of toluene SOA formed at low  
 1016 RH. Viscosity was predicted with different mass loadings ranging from 1-1000  $\mu\text{g m}^{-3}$ . Markers  
 1017 and shaded boxes represent experimentally measured viscosity values. Song et al. (2016) mass  
 1018 loadings were 60-100 and 600-1000  $\mu\text{g m}^{-3}$ . Bateman et al., (2015) and Li et al., (2015) mass  
 1019 loadings were 30-50  $\mu\text{g m}^{-3}$  and 44-125  $\mu\text{g m}^{-3}$ , respectively.  
 1020